

A real-time transient detector and the Living Swift-XRT Point Source catalogue.

P.A. Evans^{1*}, K.L. Page¹, A.P. Beardmore¹, R.A.J. Eyles-Ferris¹,
J.P. Osborne¹, S. Campana², J.A. Kennea³, S.B. Cenko^{4,5}

¹*School of Physics and Astronomy, University of Leicester, Leicester, LE1 7RH, UK*

²*INAF, Osservatorio Astronomico di Brera, via E. Bianchi 46, 23807 Merate, Italy*

³*Department of Astronomy and Astrophysics, Pennsylvania State University, 525 Davey Lab, University Park, PA 16802, USA*

⁴*NASA Goddard Space Flight Center, 8800 Greenbelt Road, Greenbelt, DMD 20771, USA*

⁵*Joint Space-Science Institute, University of Maryland, College Park, MD 20742, USA*

Accepted – Received –

ABSTRACT

We present the Living *Swift*-XRT Point Source catalogue (LSXPS) and real-time transient detector. This system allows us for the first time to carry out low-latency searches for new transient X-ray events fainter than those available to the current generation of wide-field imagers, and report their detection in near real-time. Previously, such events could only be found in delayed searches, e.g. of archival data; our low-latency analysis now enables rapid and ongoing follow up of these events, enabling the probing of timescales previously inaccessible. The LSXPS is, uniquely among X-ray catalogues, updated in near real-time, making this the first up-to-date record of the point sources detected by a sensitive X-ray telescope: the *Swift*-X-ray Telescope (XRT). The associated upper limit calculator likewise makes use of all available data allowing contemporary upper limits to be rapidly produced on-demand. These facilities, which enable the low-latency transient system are also fully available to the community, providing a powerful resource for time-domain and multi-messenger astrophysics.

Key words: Catalogues: Astronomical Data bases – Transients – X-rays: General – Astronomical instrumentation, methods, and techniques

1 INTRODUCTION

Serendipitous source catalogues have an important function in X-ray astronomy, helping us to constrain the population of X-ray emitting objects, identify new phenomena not intentionally targeted by observations and characterise the time-dependence of the X-ray sky. Such is their value that a source catalogue is a standard product of most imaging X-ray telescopes, e.g. *ROSAT* (White et al. 1994; Voges et al. 1999; Boller et al. 2016); *XMM-Newton*; (Saxton et al. 2008; Watson et al. 2009; Rosen et al. 2016; Traulsen et al. 2019); *Chandra* (Evans et al. 2010) and the *Neil Gehrels Swift Observatory* (Puccetti et al. 2011; D’Elia et al. 2013; Evans et al. 2014, 2020b). Some of these (e.g. *Chandra* and the *XMM* pointed catalogues) are narrow-field but deep; others (the *ROSAT* all-sky survey [RASS], the *XMM* slew survey, and the much-anticipated *eROSITA* (Predehl et al. 2021) catalogues) are all-sky but with less sensitivity.

The compilation of *Swift* X-ray telescope observations lies between these two extremes, covering over 12% of the sky, with

typically more sensitivity than the all-sky surveys: in the 2SXPS catalogue Evans et al. (2020b), we reported a median 0.3–10 keV source flux of 4.7×10^{-14} erg cm⁻² s⁻¹, not much above the value from 3XMM-DR8 (2.2×10^{-14} erg cm⁻² s⁻¹, 0.2–12 keV). Additionally, *Swift* typically observes a given object multiple times, giving a powerful insight into the variability of the X-ray sky. This combination of sensitivity, sky area and variability information is likely to remain unique until the multi-year *eROSITA* catalogues are published.

However, there is a drawback to typical X-ray catalogues: they are always out of date¹. Due to the time it takes to process the data, compile the results, create a database and/or interface for catalogue access, and document everything, the newest data are often at least a year old by the time the catalogue is released and the observatory has collected more data in the meantime. For many purposes, this does not matter, but with the recent growth of time-domain and multi-messenger astronomy, having an up-to-date catalogue is increasingly important. For example, when observing a new gravi-

* pae9@leicester.ac.uk

¹ Except those created after a mission has ended.

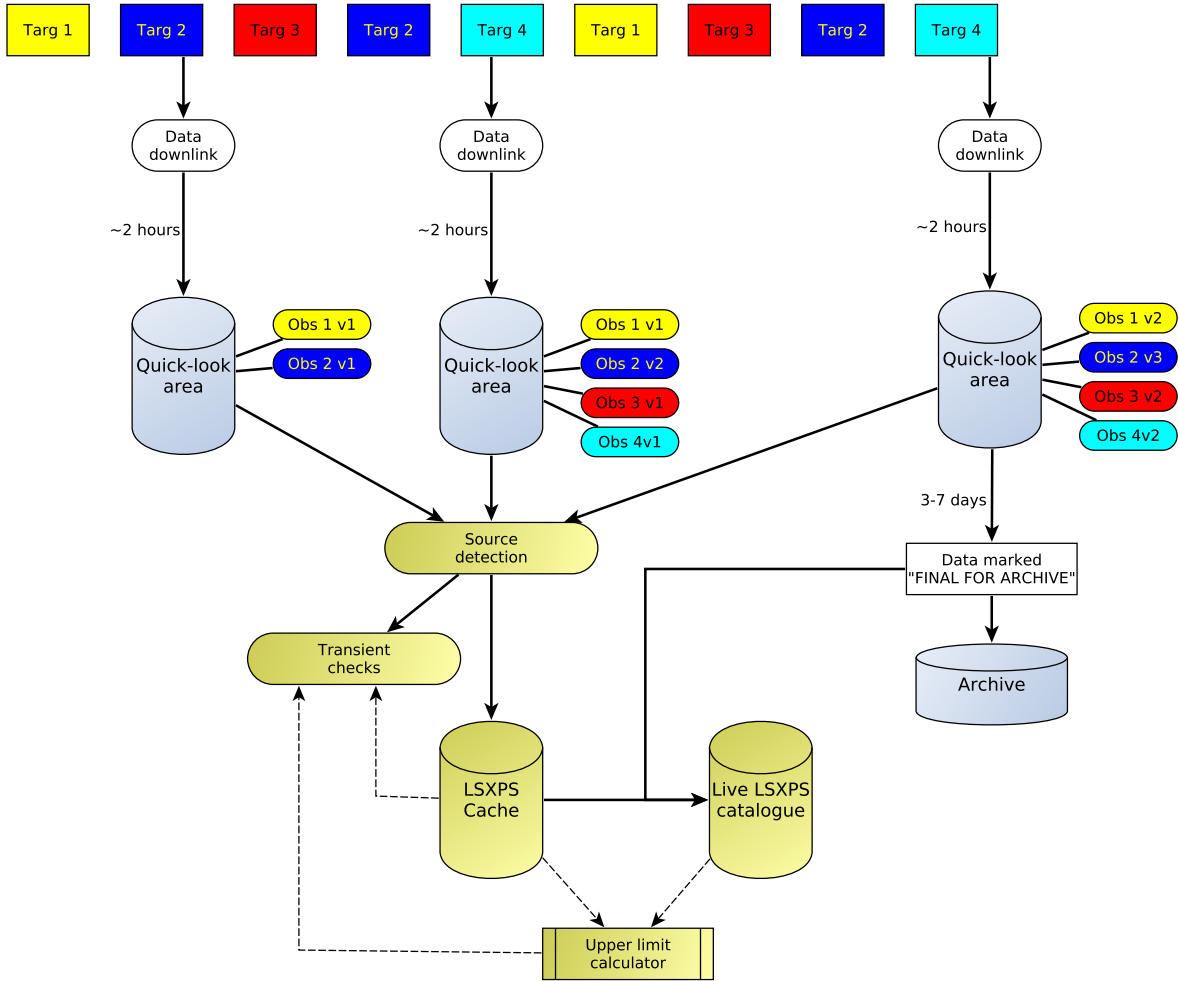


Figure 1. A simplified schematic of the *Swift* data flow. The top row shows a timeline of *Swift* pointings in a given day, each box represents a pointing with *Swift*, multiple boxes with the same colour and label are multiple pointings at the same object (‘snapshots’). Solid lines show data flow; dashed lines show data access.

tational wave event, *Swift* regularly finds new X-ray sources, but to reliably determine which (if any) is related to the triggering event requires prior knowledge of that sky location either to identify the source as a known object, or to determine whether it is above historical upper limits (Klingler et al. 2019).

Additionally, transients can be found serendipitously in X-rays; for example, the fast X-ray transients found in *Chandra* data (e.g. Jonker et al. 2013; Bauer et al. 2017; Quirola-Vásquez et al. 2022). These were found by mining the data, but were already years old by the time of their discovery, preventing rapid follow up and thus hampering the ability to expose the phenomenology of the transient, and the underlying physics. Further, the variability timescales on which such transients can be studied are limited to either the (hours to days) timescale of the discovery observation (e.g. the fast X-ray transients, or nuclear quasi-periodic eruptions, Miniutti et al. 2019; Giustini et al. 2020), or potentially to much longer timescales on which follow up can be carried out (e.g. Starling et al. 2011; Strotjohann et al. 2016). In contrast, low-latency announcement of transients allows rapid, multi-wavelength follow up to probe the nature of the transient object, and enables ongoing observations which can probe the source’s behaviour on timescales of days to

weeks/months. The scientific value of such low-latency announcement and response is well demonstrated by the case of SN2008D. This supernova occurred in the same galaxy as another supernova (SN2007uy) which was being regularly observed by *Swift*, and its sudden appearance in the X-rays was spotted by Soderberg et al. (2008). This rapid discovery enabled targeted observations of what proved to be the first X-ray detection of the shock breakout from a supernova.

Swift-XRT is an excellent tool for searching for new, serendipitous X-ray transients. Its combination of good effective area and low background, combined with *Swift*’s unique observing strategy and the rapid availability of its data, allow us to look for transients in near real-time, with sensitivity to much fainter transient events than from typical wide-field detectors such as the RXTE All Sky Monitor (Levine et al. 1996), or MAXI (Matsuoka et al. 2009).

In this work we present the ‘Living’ *Swift*-XRT Point Source (LSXPS) catalogue and real-time transient detector. Software developed and running at the UK *Swift* Science Data Centre (UKSSDC) at the University of Leicester is executed each time new *Swift*-XRT data are received. Those data are searched for new transients, and added to the LSXPS catalogue, meaning it is kept up-to-date in

nearly real-time. The provision of the real-time catalogue is essential to the transient search: a reference image is needed to determine whether a source just detected is already known in X-rays, and if not, what upper limit can be placed on its historical flux. Because *Swift* often reobserves locations on the sky (and a single XRT snapshot is usually more sensitive than the RASS or *XMM* Slew Survey observations) it is commonly the case that the best reference image to use is a previous *Swift* dataset, which is now always available in LSXPS.

2 DATA FLOW, FROM *Swift* TO LSXPS

In order to understand the ‘living’ nature of LSXPS and the latencies associated with transient detection, it is necessary to briefly introduce the structure and delivery of *Swift* data. A key and novel feature of *Swift*’s observing strategy is that it is always observing²; when a target goes into Earth eclipse, *Swift* immediately slews to the next target in its observing plan. Due to its low-Earth orbit, the longest continuous observing window is $\sim 2,700$ s and for operational reasons these are usually no longer than 1,800 s. This means that *Swift* both observes many targets during a day and that the same target may be observed multiple times on different orbits, with observations of other targets taking place in between. These individual pointings of a given target are referred to as *snapshots*, and (ordinarily³) all snapshots of a given target within a single UT day are collected together on the ground into a single *observation*: the basic data unit used for archiving and data access. Each observation is identified by its unique 11-digit obsID.

Swift typically has 8–12 ground-station contacts per day, and (again, unlike most missions) the downlinked data are made available rapidly⁴ via the quick-look sites in the USA, UK and Italy. These data are not necessarily ‘complete’: not all snapshots in a given observation may have occurred by the time of the downlink, or not all observed data may have been downlinked during the pass. With each subsequent ground-station pass, observations may be updated and the data on the quick-look site replaced with a revised (more complete) version; to track this, metadata indicates how many times the observation has been processed. Eventually, each observation will be marked as ‘complete’ by the Swift Data Center (SDC), normally 3–7 days after the data were collected. The quick-look sites will label the data as ‘FINAL FOR ARCHIVE’, and shortly thereafter these data are moved from the quick-look area to the archive.

A simplified pictorial representation of this is given in Fig. 1. The coloured boxes on the top row represent consecutive pointings; ground station passes are shown with the state of the quicklook site after each pass.

2.1 Adding data to LSXPS

Quick-look XRT data are by definition incomplete, and can also occasionally be ‘incorrect’, in the sense that the incomplete house-keeping data can result in the pipeline processing inadequately filtering the data. For this reason, observations are not added to the actual

LSXPS catalogue until they are marked as ‘complete’ by the SDC. Analysis of these incomplete observations is, however, extremely important for transient detection; not just for the obvious reason of finding transients as early as possible, but also to provide the most complete possible set of reference images for future searches⁵.

For this reason, observations are analysed each time data are received by the UKSSDC quick-look site, as shown in Fig. 1. The receipt of quick-look data triggers the LSXPS source detection, and the results are stored in a cache area which it not made publicly available. Transient checks (Section 4) are immediately carried out for each detected object and the XRT team are notified of any transient candidates, but none of the sources found in the observation, nor the observation itself, are added to the public catalogue (although the observation is available to the upper-limit server, Section 6). The transient checks for subsequent observations can make of use these cached data. When a revised version of an observation is received on the UK quick-look site, it is analysed and the cached results for the observation are replaced with those from this new analysis. In order to track this evolving situation, for LSXPS we index data not by the ObsID, but by a new property, the *DatasetID*. This is simply an incremental integer number starting from 1, and each new version of an observation is given a new DatasetID, so ‘Obs 1 v1’ and ‘Obs 1 v2’ in Fig. 1 will have different DatasetIDs⁶. Once the observation is marked as complete, the cached analysis is merged into the catalogue (see Section 3.2).

2.2 Targets, observations; stacked image definition and evolution

Swift observations are planned in terms of *targets*, where a target, with a unique targetID, corresponds to a pointing location on the sky. Thus multiple observations of the same target will share a targetID; indeed, the 11-digit obsID is just the 8-digit targetID followed by a 3-digit number tracking how many times the target has been observed. Occasionally, either due to a human error or an inaccurate slew, two observations with the same targetID have significantly different pointings; if observations with the same targetID are more than $6'$ offset from each other then within LSXPS we define new targetIDs for each of these pointings, with observations being assigned to the targets as appropriate.

As with the previous SXPS catalogues, as well as analysing individual observations, we also create *stacked images*, where all observations of the same portion of the sky are combined to maximise the exposure⁷. A stacked image is defined as a specific set of overlapping targets (or a single target, with multiple observations), and the population of stacked images is created such as to produce the minimum number of stacks while ensuring that every observation and every overlap between observations is included in at least one stack. As in the previous catalogues, stacked images are assigned fake obsIDs, incremental numbers beginning with 10^{10} , and

⁵ For example, imagine *Swift* observes the field of a new GRB and finds no new serendipitous transient. The GRB is re-observed the following day – before the first observation is marked as complete. If X-ray sources are found in this second observation, the analysis of the first observation is vital to determine if any of these sources are new transients.

⁶ DatasetIDs are set simply by the order in which data are processed; thus two different version of the same observation will not normally have consecutive DatasetIDs.

⁷ We slightly increased the maximum size of a single stacked image to 2,700 pixels ($106'$) to a side for LSXPS.

² More accurately, nearly always: it does not observe while passing through the Southern Atlantic Anomaly or slewing; due to its rapid slew speed, the latter is not a significant factor.

³ For technical reasons, sometimes an observation may span multiple days, or there may be multiple observations in one day.

⁴ Typically within about 2 hours of the downlink.

the term *dataset* is a generic term covering individual observations and stacked images.

In the previous catalogues, stacked images were statically defined, but this is clearly not possible for a living catalogue: not only are new stacks being constantly added, but the existing stacks can be modified. This can happen in two ways. First, a new observation may be taken of a target in a stack. In this case, the LSXPS processing does not change the ‘ObsID’ of the stack, but does assign it a new DatasetID (how many times this stack has been analysed is also recorded); this is deliberately analogous to what happens to single observations when they are updated with more data. Second, a new target may be observed which overlaps an existing stack. In this case, the definitions of the stacks are updated. It is impossible to say a-priori what the outcome of this will be. In the simplest case a new stack is defined which is the same as an old stack but with the new target added; however, the effect may be that the addition of the new target causes a stack to grow beyond the 2,700-pixel limit in which case multiple new stacks may be defined, or the new target may bridge a gap between two existing targets and so be able to merge all of their data into a single (new) stack. In either case, stacks that are superseded are marked as such, and are not analysed when new data are received. The handling of superseded stacks is discussed further in Section 3.3.

2.2.1 Analysing stacks

Stacks can take much longer to analyse than single observations – the runtime scales approximately with the number of snapshots – and in the most extreme cases stacked image analysis can take many weeks to run and its temporary disk usage can near a terabyte. It is thus impractical to simply run stacked analyses whenever new data are received, as is done for observations. Further, there is less need for this: as a general rule, each new observation of a stack adds only a (ever-decreasing) fractional increase in exposure time, and we do not search stacks for transients (Section 4) – their primary function for transients being the provision of historical upper limits. Therefore, stacked image processing is instead managed by a `CRON` job. This checks how many stacked image analyses are in progress, and if it is above some threshold⁸ it will terminate without submitting any new jobs. Otherwise, it identifies n observations (where n is again a tunable parameter) which were marked as complete at least 24 hours ago and have not yet been subjected to stacked analysis, finds all stacks that these observations contribute to, and triggers the analysis of those stacks. This analysis will include all observations in the stack which are marked as complete.

Long-running, high disk-usage processes are still an issue for this approach, since they can fill up all of the available stack-processing ‘slots’, causing the `CRON` job to exit without scheduling any new fields for days or even weeks. To avoid this, every time a stacked image is analysed the runtime is recorded in a database. Stacks which took more than 24 hours to run (or which supersede a stack which took more than 24 hours) are not handled by the routine `CRON` job just described, but are instead flagged in the database, and analysed at a lower cadence (loosely connected to the runtime) in a separate queue, as resources allow. By definition, these slow-running fields already contain a lot of data, therefore the

⁸ Both this threshold, and the frequency with which the `CRON` job runs are tunable parameters, allowing us to change things as our compute capacity varies.

Table 1. The warning flag bits in the detection flag; taken from Evans et al. (2020), table 4.

Bit	Value	Meaning
2	4	Source is within the extent of a known extended source.
3	8	Source likely a badly-fitted piled-up source.
4	16	Position matched area flagged by manual screening.

Table 2. The definition of the dataset warning flag, taken from Evans et al. (2020), table 5.

Bit	Value	Meaning
0	1	Stray light was present, and fitted.
1	2	Diffuse emission identified.
2	4	Stray light badly/not fitted.
3	8	Bright source fitting issues ¹

¹ i.e. the field contained a source that was heavily piled up in one band, but not fitted as such in another band. See section 3.7 of Evans et al. (2020b) for details.

incremental changes are small and the impact of this low-cadence update is minimal.

3 CATALOGUE CONSTRUCTION

The basic processing of a dataset for LSXPS remains almost the same as in 2SXPS (Evans et al. 2020b) and is not described in detail here: a brief overview is given in Appendix A and the interested reader is encouraged to read the 2SXPS paper for full details; all we will do here is to restate the four energy bands used in LSXPS:

- **Total:** 0.3 – 10 keV
- **Soft:** 0.3 – 1 keV
- **Medium:** 1 – 2 keV
- **Hard:** 2 – 10 keV

and reproduce details of the source classification system. Sources are allocated a detection flag based on their statistical properties, these can have values of *Good*, *Reasonable* and *Poor* (in the database tables, these are numerical values of 0, 1, 2 respectively). The thresholds for these parameters were set such that the fraction of spurious sources in a given sample of objects is 0.003, 0.01 and 0.1 if that sample includes *Good*, *Good* and *Reasonable* or all sources respectively; individually the classifications correspond roughly to 3-, 2- and 1- σ significance. The spurious source rate will be considerably higher in the presence of artifacts such as stray light, or an extended/diffuse source. For this reason, objects which are affected by such things (identified either automatically or by the manual screening, Section 3.1) have extra warning flags set; on the website this is shown as descriptive text; in the database these flags are bitwise values in the detection flag, as shown in Table 1. Datasets likewise have flags assigned to them to warn if there is a potential issue affecting the dataset as it is possible (but unlikely) that these issues could alter the spurious detection fraction even among objects in that field with none of their warning flags set. This flag is also a binary flag, detailed in Table 2.

There is one small but important extension to the 2SXPS algorithm for LSXPS for individual observations: the search for new transients, which is described in Section 4.

LSXPS consists of all XRT data with at least 100 s of Photon Counting (PC) mode exposure remaining after the standard XRTPIPELINE processing at the UKSSDC, and after the removal of times affected by bright Earth or unreliable pointing (Appendix A). These data are split into snapshots, only snapshots with at least 50 s of exposure are accepted⁹. All XRT data meeting these criteria were reprocessed with HEASOFT v6.29, and the XRT CALDB v20210915¹⁰ and then the catalogue creation software was run on all historical data (we did not copy the results from the earlier catalogues). This processing ‘caught up’ with the archive data towards the end of 2022 March, and after a series of short ‘catch-up’ runs, the ‘live’ processing software to handle new quick-look data as described above was enabled on 2022 April 1¹¹. The analysis of the stacked images built from historical data was also enabled at this point, with the queue of images to process automatically updated by the LSXPS processing as new data were received and so new stacks defined. Once the stacked image processing was up-to-date¹², the CRON job described in Section 2.2.1 was activated.

While the source detection algorithm is almost unchanged from 2SXPS, the aggregation of the results to form the final catalogue required significant modification for LSXPS. The method by which the various detections are rationalised to a unique source list is unchanged (see section 3 of Evans et al. 2020b), but for 1/2SXPS this step was done once, after all datasets had been processed and the list of detected objects was final. For the dynamic LSXPS catalogue this is a continuous process, and takes place when the dataset is added to the already-existing catalogue. For observations this is done when the data are marked as complete; for stacks this step is carried out immediately after the dataset processing is completed.

There are four steps involved in adding a dataset to LSXPS, which are:

- (i) Manual screening of the field[†].
- (ii) Creating a new entry in the datasets table.
- (iii) Incorporating the objects detected in the dataset into LSXPS.
- (iv) Handling older versions of a stacked image[†].

Items marked with [†] may not take place for all fields. With the exception of item (ii) (which is just a database operation), these operations are described in the following subsections.

3.1 Manual screening of fields

In order to make the quality of LSXPS as high as possible, the analysis software identifies datasets in which the results may be

⁹ This can result in LSXPS datasets with only 50 s of exposure, for example if the original 100 s of usable data was spread over multiple snapshots, only one of which exceeded 50 s in duration. This was true of the previous SXPS catalogues but has not been explicitly stated before.

¹⁰ At the time of writing, all LSXPS data use these software and CALDB versions; however, they will doubtless be updated again in the future at which point only new data in LSXPS will use the newer software and calibration: we have no plans to periodically rebuild LSXPS from scratch following such updates.

¹¹ I did consider delaying by one day. . .

¹² Or *almost* up to date. Various technical challenges were encountered relating to certain stacks with very long (> 100 hour) runtimes, almost all of which cover the Galactic centre. Analysis of these images was deferred until the backlog was cleared, and is now – slowly – catching up.

unreliable and flags these for human inspection, which must be completed before the dataset can enter the catalogue. There are two criteria that trigger this flagging.

The first of these relates to stray light and is not applicable to stacked images. X-rays from a source $\sim 30\text{--}80'$ from the XRT boresight (and so out of the field of view), can be diverted onto the XRT detector via a single reflection off the hyperbolic mirror surface; if the source is bright enough this can cause a pattern of concentric rings to appear on the XRT detector, which can give rise to spurious detections. We developed a technique to identify and fit this emission for 2SXPS (see Evans et al. 2020b, appendix A), but this is not infallible, especially if there are real X-ray sources in or near the stray light. Such errors are immediately obvious to the human eye, so any field for which the automated system deemed stray light to be present is marked for human checking. Once this dataset is marked as ‘final’, the XRT team are notified and directed to a web interface which allows them to compare the image with the fitted background model (which includes the stray light), and to either accept the model, mark the stray light as not being present (i.e. a spurious fit), or mark it as badly fitted and provide a better input position for the source of stray light. In the first case, the dataset is accepted into LSXPS. In the latter two cases, the dataset is reanalysed (reusing its existing DatasetID, as the underlying data have not changed), i.e. with stray light modelling disabled or with the new input parameters as appropriate. As soon as this reanalysis is complete, the field is again marked for screening. In the vast majority of cases it is then accepted into the catalogue. In a small number of cases, the catalogue software is not able to produce an adequate model for the stray light. In this case the XRT team will define an artifact (see below) covering the parts of the image affected by stray light, causing all detections therein to be flagged. As described in appendix A of Evans et al. (2020b), stray light is not fully fitted to stacked images; instead the results of the fits to the observations making up the stacked image are taken and applied to the stacks, with only the normalisation allowed to vary. For this reason, if the stray light fitting for a stack is poor, this must be handled by the creation of artifacts, as below.

The second reason for human verification of a dataset is if median inter-source distance in the dataset is less than $80''$. This can simply indicate a full or crowded field, but it can also indicate problems such as badly- or unfitted stray light, instrumental artifacts such as residual contamination by bright Earth or hot pixels/columns/rows in the detector, or an area of diffuse emission which is not handled by our point-source detection system and so causes spurious detections. Such fields are flagged and the XRT team again notified and directed to a website where they can investigate the image. If there is evidence of a problem, they will define a circular or elliptical region, or a set of regions, and all of the objects inside these and in this specific dataset have a warning flag applied to them. If the ‘problem’ is astrophysical in origin (as opposed to being of instrumental origin), e.g. an extended source, then the team member will mark these artifacts for propagation, which will mean that they are automatically applied to all future observations of these location on the sky. This helps to reduce the number of fields needing screening, since fields are only marked for inspection if the median distance between sources *that have not already had their warning flag set* is below $80''$.

For datasets corresponding to observations in the 2SXPS catalogue, the results of the human screening of those data in that catalogue were automatically applied where possible. That is, if the automatic stray light model closely corresponded to that accepted for 2SXPS, it was accepted for LSXPS. Artifacts identified in 2SXPS

were automatically applied to their corresponding LSXPS fields, and those fields were therefore only flagged for LSXPS screening if the unflagged sources has a low median separation.

3.2 Adding sources to LSXPS

When a dataset is added to LSXPS, the objects detected in that dataset are compared with the sources already in LSXPS. An object is deemed to match a source in LSXPS if their positions – including astrometric uncertainty – agree at the $5\text{-}\sigma$ level¹³. There are three potential results for each new object:

- (i) The object has no counterpart in LSXPS.
- (ii) The object is an additional detection of a source in LSXPS.
- (iii) The object matches an LSXPS source, but improves the position of the LSXPS source (i.e. its position uncertainty is smaller than that currently in LSXPS).

The first two are straightforward: in case (i) the object is a new source which is added to LSXPS; in case (ii) the products and average properties of the existing source are updated to include the results from the new dataset.

Case (iii) is more complex as there are several possible permutations. In the simplest scenario, the new position is identical to the LSXPS position¹⁴, but the uncertainty is smaller. Here, the catalogue entry is updated to use this smaller error and the processing continues as per case (ii), above. If, however, the new position is different from the LSXPS position, the situation is more complex as the association between individual (per-dataset) detections and LSXPS sources may change. For example, if there are several X-ray sources close together on the sky, then moving one of these sources $1''$ to the East could result in some detections previously assumed to be this source now being better associated with a different object; or indeed the inverse. On the other hand, if a source position is revised it may now be the case that some of the detections, which had been attributed to that source, are not consistent with the new position, nor are they consistent with that of any existing source; i.e. the original ‘source’ is now found to be two distinct sources, which of course each need a record in LSXPS.

In order to identify and handle all of these cases, when a dataset is added to the catalogue we select every LSXPS source that lies within the field of view of the new dataset, and every individual detection of those sources; then we find any other sources within $5\text{-}\sigma$ of those detections, and all detection of these; and so on recursively until no extra objects are found. This is analogous to picking up a paperclip with a magnet and so also retrieving all connected paperclips until a gap (in this case, a $5\text{-}\sigma$ gap) is found, and essentially ensures that we collect every single detection in any dataset and band that could potentially be affected by the new dataset. We then apply the source matching algorithm from 2SXPS (Evans et al. 2020b section 3.7) to this subset of detections. This yields the list of unique sources and which detections are associated with each, and the catalogue is revised accordingly. If a source moves such that its name changes, a new entry is created in the catalogue and the old entry deleted, but a record of this is kept. Records are also kept of which sources are deconvolved into multiple

sources, and which individual detections are reassigned from one source to another. This book-keeping is extremely important for the usability of a dynamic catalogue such as LSXPS: if someone studies a particular source, perhaps announcing it to collaborators or the wider community, and then the source disappears without a trace this would be very unhelpful! The user interface (Section 6) ensures that if a user requests a ‘superseded’ source they will either be redirected to the new entry which has replaced this source, or if necessary presented with a list of the sources into which it has been deconvolved.

3.2.1 Source products and updates

For each source, a series of products and measurements are created, and these are the same as in 2SXPS (see Evans et al. 2020b, section 4). In short, these comprise mean count-rates in each energy band; two time-averaged hardness ratios; and light curves of all energy bands and hardness ratios, with one bin per observation, and one bin per snapshot. Unlike some catalogues, these light curves and count-rates are fully corrected for effects such as pile up, vignetting, dead columns on the detector etc. and so can be used with no further corrections needed. A measurement of variability using the Pearson’s χ^2 is calculated for each time series. The two hardness ratios are defined as:

$$\text{HR1} = (M - S)/(M + S) \quad (1)$$

$$\text{HR2} = (H - M)/(H + M) \quad (2)$$

where S, M, H refer to the background-subtracted count-rates in the soft, medium and hard bands respectively.

Spectral and flux information is also provided for each source, with up to three methods employed per source, depending on the characteristics. Two spectral models are used: an absorbed power law, and an absorbed optically thin plasma model (APEC; Smith et al. 2001); absorption was calculated using the TBABS model (Wilms et al. 2000). Flux conversions and (where appropriate) spectral properties were derived using XSPEC. For every source, fluxes were deduced using fixed spectral components: a power law with photon index 1.7 and an APEC with a plasma temperature of 1 keV; the absorption column was set to the Galactic value along the line of sight to the source, from Willingale et al. (2013). These values are available for every source but are the least accurate since they simply assume the spectral shape, regardless of the data. Where possible, the spectral parameters and flux are also inferred from the hardness ratios, using look-up tables linking (HR1,HR2) to the model parameters – for full details see Evans et al. (2020b) section 4.1 and Evans et al. (2014) section 4.2. For sources with at least 50 net counts in the total band, and a detection flag of *Good* or *Reasonable* (Section 5) with no stray light or diffuse source warning set, we also extract and fit a spectrum. This is done using the tools of Evans et al. (2009), and we fit both absorbed power-law and APEC models.

As LSXPS is a living catalogue, these source properties are not static. Every time a new dataset is added to the catalogue, all sources that lie within the field of view of that dataset (regardless of whether or not they were detected in it) have their products updated.

¹³ More correctly, at the probability associated with a Gaussian $5\text{-}\sigma$ confidence. Since the radial position errors should follow a Rayleigh distribution, this level was determined based on Rayleigh, not Gaussian, statistics.

¹⁴ We define ‘identical’ as meaning, ‘does not change the IAU-format name of the object’, where the IAU format is “LSXPS JHHMMSS.S±ddmmss”.

3.3 Handling older versions of a stacked image

When a new version of a stacked image is added to the catalogue it is preferable to remove the old version, rather than keeping large numbers of obsolete datasets. If every source detected in the old version is also detected either by the new version, or by another dataset, then there is no reason to keep the old version of the stacked image. Its data are removed from disk and from most of the database tables¹⁵. It can happen, however, that a source is detected in a stacked image, but not in the updated version of that stack – especially for faint and variable or transient sources. If the old version of a stacked image contains the only detection of a source in LSXPS, that stacked image will not be removed from the catalogue. Instead, the source is flagged internally as an ‘orphan’, and the dataset is marked as being an ‘obsolete stack’. Should an orphan source ever be detected in a new dataset (single observation or stacked image), its orphan status is removed; should this happen to all orphans in an obsolete stack, that stacked image is then removed. The same process is followed when a new stacked image is analysed which supersedes a stack currently in the catalogue; that is, the new stack has a different definition (and obsID), but contains all of the targets in an old stack (see Section 2.2).

3.4 Static catalogue releases and data reprocessing

The introduction of a living catalogue, with near real-time updates, does not remove the need for ‘static’ catalogues, for projects which require a stable and unchanging reference such as where the reproducibility of a project is crucial. It is therefore our intention to issue frozen releases of the catalogue (3SXPS, 4SXPS, etc.) at regular intervals, likely every 1 or 2 years. These will essentially be ‘snapshots’ of LSXPS, but will be full decoupled from LSXPS, so completely insulated from updates. Because of the timescales on which stacked image analysis runs, it may not be possible to fully ‘synchronise’ the contents of these releases; that is, to ensure that the stacks in a static release contain all of the observations in the release, and only those observations. We do not see this as a major issue, as the key point of these releases is that their contents can be quantified and are unchanging, and this will be ensured. The first static release, 3SXPS, is envisioned for 2023.

Before building LSXPS, we reprocessed all historical XRT data with what was, at the time, the most recent HEASOFT and XRT calibration releases (Section 3). However, these are regularly updated¹⁶ and calibration in particular is, by its nature, always retrospective. While the UKSSDC does periodically reprocess the entire XRT archive following such updates, we are not planning to rebuild the LSXPS catalogue following such processing. The CALDB and HEASOFT versions used in the live LSXPS analysis will be updated, but the data already in the catalogue will not be revised. The reason for this is that such a revision would essentially involve completely rerunning the LSXPS analysis: a process that takes around 6 months and monopolises compute time, and so clearly cannot be done routinely! It is not anticipated that any software or calibration revisions will have a major impact on the catalogue contents¹⁷. Changes in the XRT gain could potentially have a (very) small impact on

the hardness ratios and spectral properties of sources; however, the catalogue web pages and the API (Section 6) are fully integrated with the UKSSDC software to provide high-quality analysis of point sources (Evans et al. 2009), making it easy to generate custom spectral products for sources of interest, making use of the latest software and calibration, and using the archive data locally reprocessed with these at the UKSSDC.

4 TRANSIENT DETECTION AND CLASSIFICATION

We define a serendipitous transient as an object which is uncatalogued in X-rays, has a flux above historical upper limits and was not the target of the *Swift* observation. In order to minimise the delay in detecting and announcing these transients we do not wait for an observation to be marked as complete before carrying out transient checks, but rather carry out these checks immediately after each analysis of an observation.

The transient checks applied to each detected object can be broken into the following steps:

- (i) determine whether the object is a known X-ray source
- (ii) determine whether it is above historical upper limits
- (iii) carry out basic analysis of the object
- (iv) classification of the object

and these steps are described in the following sections. At each step the process may terminate; e.g. if the source is a known X-ray emitter, then steps (ii) onwards are not carried out.

During the bulk processing of historical data, the transient checks were carried out, but notifications of new transients (see below) were not produced and the candidate transients were not added to the main LSXPS transients database but stored separately. This is because the events are, by definition, old and so not pressing, and may have been announced or published already. The primary purpose of enabling transient checking and analysis during the historical process was to test and debug the software and tune the automated classification process (Section 4.4); however, we may release the database of these historical transients or some analysis thereof at a future date.

4.1 Is the object an known X-ray source?

We deem an object to be uncatalogued in X-rays, if it does not correspond to a source already in LSXPS (or in the cache¹⁸), and is inconsistent at the $5\text{-}\sigma$ level with any object in the X-ray Master catalogue provided by HEASARC¹⁹, CSC 2.0 (Evans et al. 2020a) or the live XRT GRB catalogue (Evans et al. 2009)²⁰. This set of reference catalogues may be updated in future (for example, with the addition of *eROSITA* catalogues), an up-to-date list will be maintained on the LSXPS website.

4.2 Comparison with historical upper limits

We compare the flux at discovery with upper limits obtained from *Swift* itself and also *XMM-Newton* and *ROSAT*²¹. *XMM* has a sim-

¹⁵ A record of all such deleted datasets is still maintained but this is not part of the public catalogue.

¹⁶ Indeed, HEASOFT 6.30 was released during the processing.

¹⁷ In the unlikely event that something changes that is impactful, we will investigate how best to respond, and in such cases a complete rebuild of the catalogue cannot be ruled out.

¹⁸ Excluding sources found in an earlier version of the observation being analysed.

¹⁹ <https://heasarc.gsfc.nasa.gov/W3Browse/all/xray.html>.

²⁰ https://www.swift.ac.uk/xrt_live_cat

²¹ This list may also be revised in future, especially to include *eROSITA*; the LSXPS website will maintain an up-to-date list

ilar band-pass to *Swift*-XRT and we can use the total (0.3–10 keV) LSXPS band for this analysis. *ROSAT*, however, has a much softer band-pass, 0.1–2.4 keV, thus for comparison with *ROSAT* we use the combination of the soft and medium (0.3–1, 1–2 keV) LSXPS energy bands, hereafter the ‘SM’ band.

We create light curves with one bin per snapshot (i.e. *Swift* orbit) in the total, soft and medium LSXPS energy bands, summing the latter two to give the SM-band light curve. The peak per-snapshot count-rate is then identified from these light curves, defined as the bin with the highest $1-\sigma$ lower-limit²². We also calculate the mean count-rate of the object across the observation in the total and SM bands; if this has a higher $1-\sigma$ lower-limit this is instead taken as the peak rate. To enable us to compare upper limits in the next step, we also calculate the ratio, R , of the peak count-rates in the total and SM bands.

$3-\sigma$ upper limits are then obtained from LSXPS (including cached datasets and stacked images, see Section 6), *XMM-Newton* and *ROSAT*; the latter two instruments’ limits are obtained using the HILIGT service²³ (Saxton et al. 2022; König et al. 2022). Of these, only the RASS is an all-sky survey thus not all upper limits are always available. Upper limits are created in count-rate units using the native energy band of the instrument (0.2–12 keV for *XMM*, 0.2–2 keV for *ROSAT* and 0.3–10 keV for LSXPS); for *XMM* limits from both pointed and slew data are requested. These limits are then converted to XRT count rates, using fixed conversion factors determined using *PIMMS* and assuming a power-law spectrum with spectral index 1.7 and an absorbing column of 10^{21} cm^{-2} ; for *XMM* the conversions were calculated for each instrument and filter and so the appropriate one is selected. *XMM* upper limits are converted to total-band rates, and *ROSAT* limits to SM band rates. The deepest of these upper limits is then taken as the reference value to use. Since the *ROSAT* limit is in a different energy band from the others, for the comparison we multiply it by the ratio R defined above which helps to account for the spectral shape of the object, which is unknown at this point. Having determined the deepest upper limit, the peak count-rate from the appropriate band is compared with this limit, and if it is at least $1-\sigma$ above it, the object is flagged as a candidate transient²⁴.

During the historical processing, we found that all transient candidates that had a detection flag of *Poor* or one of the warning flags set (see Appendix A) were spurious detections, and indeed a significant fraction of alerts came from such objects (this is expected: a real source with a *Poor* detection is unlikely to be bright enough to pass the above tests, and while transients occurring within a stray light ring or known extended object are not impossible, they will be rare, whereas spurious detections with high apparent count-rates are much more common). Accordingly, such candidates are automatically classified as *Spurious* (Section 4.4) and the analysis (Section 4.3) is not carried out and the XRT team is not alerted to such events. They are still posted to the team-only website discussed below, and they can be ‘upgraded’ if a team member studying the image believes them to be real, but they are not routinely analysed.

²² This definition is robust against datapoints with very large errors; a count-rate of 0.5 ± 0.05 is deemed higher than a rate of 2 ± 1.9 .

²³ xmmuls.esac.esa.int/hiligt/.

²⁴ Note that the *ROSAT* limit extrapolated to the 0.3–10 keV band is *only* used for comparing with the upper limits to determine which is deepest. If *ROSAT* is selected by this test, it is the upper limit in the SM band which is used, and compared with the peak SM-band count rate.

4.3 Basic transient analysis

For each candidate transient identified by the previous steps, custom data products are built using the tools that power the UKSSDC on-demand analysis services²⁵ (Evans et al. 2009). A light curve is built using all available XRT data, including those taken before the transient discovery (if available); this can result in evidence of historical emission from the source even though it has not been previously detected, since forced-photometry at the location of a known source is more sensitive than a blind search²⁶. This is binned in three ways: with fixed numbers of counts per bin, with one bin per snapshot, and with one bin per observation. A spectrum is also created using only the discovery observation; this is partly to maximise the S/N, and also to determine the spectral state specifically at the moment of outburst. This spectrum is automatically fitted with an absorbed power-law model, and if the automatic fit is successful and the reference upper limit (Section 4.2) is not from LSXPS, then the upper limit is revised, the conversion from *XMM* or *ROSAT* to XRT being recalculated with this fitted model, using *PIMMS* and the best-fitting model parameters.

These data products and the revised upper limit are posted to a website accessible only to the XRT-team, who are then notified by email of the potential transient and asked to confirm its status and classify it. This happens even if the redetermined upper limit is no longer below the peak count-rate, in case the spectral fit was poor; however the notification email does indicate if this was the case.

4.4 Transient classification

The final step of transient analysis requires human checks to filter out objects which are definitely not serendipitous transients, and to further classify those which are. This step is currently semi-automated: the analysis system tries to suggest a classification, but a human is still required to verify or change this before the transient is made public.

Objects may be deemed not to be serendipitous transients for the following reasons:

- **Spurious detection:** the ‘transient’ may be an obviously spurious detection. Many of these cases are identified automatically as noted above but some may not be – for example if the X-ray ‘source’ is actually an artifact of optical loading, the automated system will (usually) warn that this is possible, but will not automatically flag the source as spurious.
- **Targeted transient:** the object is a transient, but is not serendipitous, it is the object *Swift* was observing (e.g. as a target-of-opportunity observation of a transient discovered elsewhere). These cases can usually be flagged automatically by the analysis code, which uses the `OBSQUERY` class in the `SWIFTOOLS` PYTHON package²⁷ to determine what object was the target of the observation. In cases where the target observation had a large position uncertainty, the automatic flagging is less reliable.
- **It is not a transient:** analysis of the historical light curve may show a series of previous bins in which the source flux can be constrained, and is consistent with that at the time of discovery. In this case the source is clearly not transient, but as a result of the specifics

²⁵ https://www.swift.ac.uk/user_objects.

²⁶ In each bin, if the $3-\sigma$ lower-limit on the count-rate is non-zero, a ‘detection’ comprising a count-rate and $1-\sigma$ errors is produced; otherwise a $3-\sigma$ upper limit is created

²⁷ <https://www.swift.ac.uk/API>.

of the current observation happens to have been blindly detected for the first time. Alternatively, the spectral fit to the transient data may cause the historical upper limit to be above the peak flux; if the XRT team member confirms that this fit is reliable, the transient nature of the source is retracted.

There is an additional category that is not listed above, a *proprietary transient*. This is an object which passes the above tests and is a real transient, but the parent observation was part of a programme designed to monitor a specific region to look for new transients. In this case whether the transient should be deemed ‘serendipitous’ is open to interpretation, but it is clearly inappropriate for the *Swift* team to routinely and rapidly announce the primary science of someone’s approved observing programme, and before they have even had time to examine the data! In these cases, the *Swift* team will endeavour to contact the observation PI and encourage them to announce the transient, and the object will not be posted to the public transients catalogue or webpage without their consent.

Items which are not caught by the above are still not necessarily transients, and are manually classified into one of the following groups, collectively referred to as ‘interesting classes’.

- **Outburst:** If the light curve shows historical detections of the source (from the forced photometry) but at a flux level below that of the new observation, the source is likely an outburst rather than a transient.

- **Low significance:** The Eddington bias (Eddington 1940) causes objects detected close to the sensitivity limit to be preferentially recorded with count-rates significantly above their true value; this can result in sources which are in reality below the historical upper limit (i.e. not transients) to be misclassified as transients. We are not able to say a-priori whether a given source is affected by this bias, although Evans et al. (2014) (section 6.2 and fig. 10) showed that SXPS sources with fewer than ~ 30 counts are affected by this bias. Sources whose peak count-rate is $< 3\sigma$ above the $3 - \sigma$ upper limit and which have fewer than 30 counts in the detection are usually classed as *low significance*.

- **Needs follow up:** This is somewhat of a catch-all category, where the source does not obviously fall into either category above, but there is some doubt as to its nature and further observations are felt necessary before it can be definitively identified as a transient.

- **Confirmed transient:** The object is definitely a new transient.

The reader will immediately realise that these classifications are to a considerable degree subjective, and they should be interpreted as such. All events falling into these categories are made publicly available (Section 4.5) and the classifications are intended as a guide and to enable filtering, rather than a definitive statement; this also helps the clear candidates to be easily identifiable from among the (larger number of) low significance and outburst events.

The *outburst* category is particularly subjective, in that in reality the only phenomenological difference between an outburst and a transient is the sensitivity of previous observations. Two identical sources, with quiescent fluxes of (say) 10^{-14} erg s^{-1} and outburst fluxes 100 times higher, could be classed one as a transient and one as an outburst, if the latter had a historical observation long enough for forced photometry to detect it in quiescence.

Swift J051001.8-055931 presents a good case study of this subjectivity. It was discovered in observation 00014892016 (version 4, LSXPS DatasetID: 225587) which began at 23:59 UT on 2022 July 20. The light curve (Fig. 2) showed a detection in the previous observation which had been accumulated over the previ-

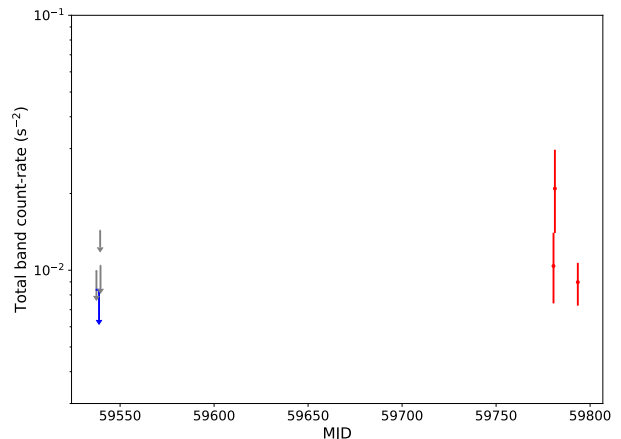


Figure 2. 0.3–10 keV light curve of Swift J051001.8-055931, one bin per *Swift* observation. The transient was discovered in the observation corresponding to the penultimate datapoint; the final datapoint comes from the follow-up ToO observations, i.e. this datapoint was not available when the transient was first reported to the XRT team. The grey upper limits are from the individual observations; the blue upper limit is the limit from the stacked image which combined these observations.

ous 16 hours²⁸, and several non-detections (grey arrows) more than 240 days earlier. At the time of the discovery, the LSXPS stacked image contained only those non-detections, from which an upper limit of 0.0084 ct s^{-1} was deduced (blue arrow); the count-rate at discovery is clearly well above the upper limit, but the automated system recommended this be classified as an outburst due to the detection in the previous observation. As the day-old ‘historical’ detection could indicate the rise of the transient, this was instead manually classified as *needs followup*. A *Swift* ToO observation was requested to investigate further; this revealed that the source, while still detectable, had dropped below the historical upper limit and thus the ‘transient’ discovery was probably either a short-lived outburst or just a low-significance fluctuation. In this case we classified it as an outburst, but *low significance* would be equally justifiable.

4.5 Transient announcement and data access

As soon as a transient is classified into one of the interesting classes (Section 4.4), it is published on the public transient webpage: <https://www.swift.ac.uk/LSXPS/transients>, and added to the public transients database (Section 5). At the present time, no push notifications are produced, although we are discussing the recording of these transients (or some subset thereof) in the Transient Name Server.

If a transient is reobserved after discovery, whether intentionally or serendipitously, its light curve is updated and also a second spectrum constructed and fitted, using all data from the discovery observation onwards. Normally these products are only updated until the discovery dataset enters the live LSXPS catalogue (Section 3), at which point the transient will correspond to an LSXPS source (and the transient page and database will contain this link), and the source products are kept up to date in the main catalogue (Section 3.2.1). However, because source products are only updated to include observations that have been added to LSXPS, they lag a

²⁸ Not accumulated continuously; that observation contained 3.2 ks of exposure gathered over the 16-hour interval.

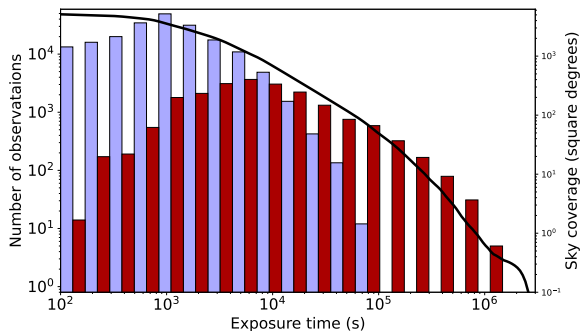


Figure 3. The sky coverage and exposure details of the LSXPS catalog as of 2022 August 30. The solid line shows the sky coverage (corrected for overlaps) as a cumulative function of exposure time (i.e. area with at least the exposure indicated). The histogram shows the distribution of exposure time per dataset, with the individual observations shown in light blue and the stacked images in red; the different colors are each half the width of the actual bins.

few days behind real time. On occasion there may be a transient for which follow-up observations have been requested and for which it is desirable to maintain up-to-date products in real time. In such cases the XRT team will manually flag the transient and its products in the transient area will continue to be updated each time new data are received. An example of such an event is Swift J023017.0+283603, a source which demonstrates the power of our new transient detector. It is consistent with the nucleus of a known galaxy and has a very soft X-ray spectrum, and so was initially announced as a probable tidal disruption event (Evans et al. 2022). Had this source only been found in later analysis, as was hitherto typical, this classification would likely have been unchallenged. However, the prompt transient alert from our new system allowed rapid and long-term multi-wavelength monitoring, exposing variability on timescales of weeks, challenging the initial classification of the object and exposing its true, and much more enigmatic, nature (Evans et al. 2022, in prep).

The transient data and database tables can be accessed through the LSXPS website and `SWIFTOOLS PYTHON` module as described in Section 6.

5 CATALOGUE CHARACTERISTICS AND CONTENTS

Being a dynamic catalogue, any statement of characteristics is obviously tied to the time at which they were generated: the ‘live’ status of the numbers given here are available on the LSXPS website. The numbers given below were obtained at 15:00 UT on 2022 August 30.

The LSXPS catalogue contains 279,021 unique sources, composed from 1.5 million blind detections across all four energy bands, or 756,769 ‘obs sources’²⁹. The median 0.3–10 keV flux (assuming a power-law spectrum) is 4.1×10^{-14} erg cm⁻² s⁻¹. The sky coverage of LSXPS is shown in Fig. 3; the total unique sky coverage is 5,186 deg², 3,503 deg² have at least 1 ks of exposure and

²⁹ An ‘obs source’ is produced by merging all detections of the same object across the energy bands within a single dataset; this is analogous to what the *XMM* catalogues call a detection.

~ 700 deg² have been observed with at least 10 ks. The 2SXPS catalogue contained data up to 2018 August 1; thus on average LSXPS has grown by 49 sources per day and the unique sky coverage is increasing at 0.94 deg²/day.

The source detection mechanism employed for LSXPS was the same as for 2SXPS, and so only summarised here. For full details see Evans et al. (2020b), especially sections 3.5 and 7, figs. 6–7 and tables 3 and 6.

As for 2SXPS, we provide ‘clean’ and ‘ultra-clean’ subsets of the sources and dataset. Clean sources are those with a best detection flag of 0 or 1 (i.e. *Good* or *Reasonable* with no other warning bits set); `OpticalLoadingWarning`, `StrayLightWarning` and `NearBrightSourceWarning` all unset; and a field flag of 0 or 1 (see Table 2). Ultra-clean sources are a subset of the clean sources, with detection and field flags of 0. There are 190,902 clean sources and 170,372 ultra-clean sources in LSXPS, a growth rate of 30 (26) per day for the clean (ultra-clean) classes.

The actual catalogue contents are organised into six publicly-available tables, which are described in Appendix B.

6 ACCESS TO LSXPS: THE WEBSITE AND API

The LSXPS catalogue is available from the UKSSDC website via: <https://www.swift.ac.uk/LSXPS>. This website provides interactive tools to explore the catalogue (i.e. cone searches, filters, etc.) and visualisations of all datasets and sources and relevant properties. The catalogue tables (Appendix B) can also be downloaded from here as FITS or CSV files. Due to the dynamic nature of the catalogue, these files are updated every hour. These hourly snapshots are available via the website for one week after creation; daily snapshots are created at midnight UT each day and available indefinitely. It is thus recommended that for any serious project based on a frozen snapshot of LSXPS, one of these daily snapshots is used to enable the work to be reproducible in future.

The website also includes an upper limit calculator, as provided for the previous catalogues; the operation of this system was described in Evans et al. (2014), section 4.4. For LSXPS this server queries all data, including those still in the cache (that is, observations which are not marked as complete, see Section 2.1). The ESA HILIGHT upper limit server (Saxton et al. 2022; König et al. 2022) currently queries 2SXPS for upper limits from *Swift*, but this will soon be updated to use LSXPS.

The catalogue can also be accessed through the `SWIFTOOLS PYTHON` module. This module, which can be installed via `PIP`, contains two components, both of which are extensively documented. `SWIFTOOLS.SWIFT_TOO` is maintained by Jamie Kennea (at Penn State University) and provides functionality including access to *Swift* data, the ability to query the observability and observing history of a given object, and to submit ToO requests; it is documented at https://www.swift.psu.edu/too_api/. `SWIFTOOLS.UKSSDC` is maintained by Phil Evans, and was added in `SWIFTOOLS v3.0`. This version includes tools to access data and query different *Swift* catalogues; this includes GRB data and catalogues, and LSXPS. All functionality of the LSXPS website, including the upper limit server is available through the API, including integration with the tools that allow on-demand analysis of sources (themselves provided through the `SWIFTOOLS.UKSSDC.XRT_PRODS` module³⁰), and much of the functionality has also been backported

³⁰ Prior to `SWIFTOOLS v3.0`, this module was `SWIFTOOLS.XRT_PRODS`, and

to 2SXPS, so that this can also be queried by the module. This module is documented at <https://www.swift.ac.uk/API/>.

We ask that users of the catalogue, via the website, data tables or API, acknowledge this in their subsequent publications: by citing this paper and also including in the acknowledgements the sentence: *This work made use of data supplied by the UK Swift Science Data Centre at the University of Leicester.*

7 SUMMARY

We have presented the first-ever low-latency, sensitive X-ray point-source catalogue and transient detector. This enables rapid follow up of X-ray transients too faint to trigger all-sky monitors and so opens up a new region of transient phase-space for exploration. This is enabled by the unique provision of a ‘living’ source catalogue, LSXPS; which is kept constantly up to date every time a new *Swift* observation is marked as completed. This catalogue and associated upper limit server provide not only a reference for our transient detector, but a valuable resource for the rapidly-growing field of time-domain and multi-messenger astronomy generally, in which it is often useful to have quick access to the most up-to-date analysis of a given sky location.

ACKNOWLEDGEMENTS

For the purpose of open access, the author has applied a Creative Commons Attribution (CC BY) licence to any Author Accepted Manuscript version arising. This work made use of data supplied by the UK Swift Science Data Centre at the University of Leicester. PAE, KLP, ABP and RAJE-F acknowledge UKSA support. SC acknowledges the support from the Italian Space Agency, contract ASI/INAF n. I/004/11/5. This work is partially supported by a grant from the Italian Ministry of Foreign Affairs and International Cooperation Nr. MAE0065741.

DATA AVAILABILITY

All of the original *Swift* data are available via the three Swift datacentres: (https://www.swift.ac.uk/swift_live/, <https://swift.gsfc.nasa.gov/archive>, <https://www.ssdsc.asi.it/mmia/index.php?mission=swiftmastr>). The data derived for this paper are available through the LSXPS catalogue web pages <https://www.swift.ac.uk/LSXPS/>) and can also be accessed using the SWIFTOOLS Python module, available via PIP.

REFERENCES

- Bauer F. E., et al., 2017, *MNRAS*, **467**, 4841
 Boller T., Freyberg M. J., Trümper J., Haberl F., Voges W., Nandra K., 2016, *A&A*, **588**, A103
 D’Elia V., et al., 2013, *A&A*, **551**, A142
 Eddington Sir A. S., 1940, *MNRAS*, **100**, 354
 Evans P. A., et al., 2009, *MNRAS*, **397**, 1177
 Evans I. N., et al., 2010, *ApJS*, **189**, 37
 Evans P. A., et al., 2014, *ApJS*, **210**, 8

- Evans I. N., et al., 2020a, in American Astronomical Society Meeting Abstracts #235, p. 154.05
 Evans P. A., et al., 2020b, *ApJS*, **247**, 54
 Evans P. A., Campana S., Page K. L., 2022, *The Astronomer’s Telegram*, **15454**, 1
 Giustini M., Miniutti G., Saxton R. D., 2020, *A&A*, **636**, L2
 Jonker P. G., et al., 2013, *ApJ*, **779**, 14
 Klingler N. J., et al., 2019, *ApJS*, **245**, 15
 König O., et al., 2022, *Astronomy and Computing*, **38**, 100529
 Levine A. M., Bradt H., Cui W., Jernigan J. G., Morgan E. H., Remillard R., Shirey R. E., Smith D. A., 1996, *ApJ*, **469**, L33
 Matsuoka M., et al., 2009, *PASJ*, **61**, 999
 Miniutti G., et al., 2019, *Nature*, **573**, 381
 Predehl P., et al., 2021, *A&A*, **647**, A1
 Puccetti S., et al., 2011, *A&A*, **528**, A122
 Quirola-Vázquez J., et al., 2022, *A&A*, **663**, A168
 Rosen S. R., et al., 2016, *A&A*, **590**, A1
 Saxton R. D., Read A. M., Esquej P., Freyberg M. J., Altieri B., Bermejo D., 2008, *A&A*, **480**, 611
 Saxton R. D., et al., 2022, *Astronomy and Computing*, **38**, 100531
 Smith R. K., Brickhouse N. S., Liedahl D. A., Raymond J. C., 2001, *ApJ*, **556**, L91
 Soderberg A. M., et al., 2008, *Nature*, **453**, 469
 Starling R. L. C., et al., 2011, *MNRAS*, **412**, 1853
 Strotjohann N. L., Saxton R. D., Starling R. L. C., Esquej P., Read A. M., Evans P. A., Miniutti G., 2016, *A&A*, **592**, A74
 Traulsen I., et al., 2019, *A&A*, **624**, A77
 Voges W., et al., 1999, *A&A*, **349**, 389
 Watson M. G., et al., 2009, *A&A*, **493**, 339
 White N. E., Giommi P., Angelini L., 1994, *IAU Circ.*, **6100**, 1
 Willingale R., Starling R. L. C., Beardmore A. P., Tanvir N. R., O’Brien P. T., 2013, *MNRAS*, **431**, 394
 Wilms J., Allen A., McCray R., 2000, *ApJ*, **542**, 914

while that path is still active and supported, it now simply silently wraps SWIFTOOLS.UKSSDC.XRT_PRODS. There are excellent reasons for this, but they are very boring.

APPENDIX A: DATASET PROCESSING ALGORITHM

This appendix contains an overview of the processing of datasets in LSXPS. For a full description including details of how the various tasks are performed, see [Evans et al. \(2020b\)](#); particularly sections 2–3 and (for details of stray light modelling) appendix A.

The first step of dataset processing differs for single observations and stacked images. For a single observation, the data are filtered to remove all times potentially contaminated by bright Earth or when the spacecraft astrometry was unstable or unreliable. If this leaves less than 100-s of cleaned PC-mode data, the dataset is discarded and the processing stops – the dataset is not added to LSXPS. Otherwise, the data are split up into snapshots – times of continuous observing. This is necessary because *Swift* does not point in exactly the same direction each time it observes a given target. Snapshots with less than 50 s of PC-mode exposure are rejected (and if no snapshot has sufficient exposures, the observation is discarded); for the other snapshots the pointing direction and XRT window size are recorded, and a catalogue check is carried out to identify any bright X-ray sources outside the field of view that could potentially cause stray light patterns. Images are created for each snapshot in each of the four LSXPS energy bands, and an exposure map and total-band event list are also created. These per-snapshot results are then combined to create a summed image per energy band and a summed exposure map and event lists (the individual images and exposure maps are retained, as these are needed by the source detection code).

Stacked images are built from individual observations in LSXPS, thus the steps above do not need to be repeated. The per-snapshot images, event lists and exposure maps are simply retrieved for each observation in the stack, these are then mapped onto the WCS coordinate system of the stacked image and summed. From this point onwards the processing is identical for observations and stacked images.

The next step is source detection and characterisation: the algorithm for this is shown in Fig. A1. For each energy band, possible sources are identified by a sliding cell approach, and then localised with a PSF fit; likelihood tests are carried out to either rank them as *Good*, *Reasonable* or *Poor*, or to reject them as spurious. This process is iterative, with a background model constructed in each cycle using the information from the previous cycles; this includes adding a PSF model of each source identified so far, reducing the number of aliases and helping to deconvolve nearby sources. This background map also includes modelling any stray light in the image³¹. Once the final list of objects in the image has been produced, their positions are all redetermined (in descending order of S/N ratio) since these may be improved with full knowledge of the other sources in the image. The count-rates for each source in this image (and hence energy band) is also calculated, unlike in many X-ray catalogues, these are fully corrected for effects such as pile-up, vignetting, dead columns or pixels on the CCD etc.

There are two minor changes to the details of this process since 2SXPS. The first of these is a recalibration of the point-spread-function (PSF). This had been done for 2SXPS and the new PSF was described in appendix B of [Evans et al. \(2020b\)](#); however some small improvements were made some time after the publication of that work, and a new PSF calibration file was formally released into the CALDB by the *Swift* team³². The changes were negligible; however, we adopted the officially-released PSF for this catalogue.

The second change relates to the way in which pile up is handled in the partial energy bands. When a source is piled up the PSF will be distorted in all energy bands, regardless of the count-rate in that band: an absorbed source can have a very piled-up PSF and yet a very low count-rate in the soft band, for example. To ensure that the PSF was properly fitted in 2SXPS, we required that sources in the sub-bands that were likely counterparts to a piled-up source in the total band, be fitted with the piled up PSF (section 3.4 of [Evans et al. 2020b](#)). This sometimes still gave poor PSF characterisation or position measurement in the sub-bands, so for LSXPS we have modified this further, constraining the pile-up parameters of the PSF model in the sub-bands to be fixed at the values determined in the total band. It is still the case, as in 2SXPS, that if a piled up source is not found at all in a sub-band, but other, non-piled-up sources are found near to the position of that source in the total band, those sources are flagged as likely aliases of the piled up source, and bit 3 (value 8) of their detection flag is set (Table 1).

Once source detection is complete, the source lists from the different energy bands are combined to make a unique list of objects found in this image; this is based on spatial separation and does not use the systematic error on the XRT astrometry, since it is common to all bands. Once the list of unique objects in the dataset has been created, checks are carried out to warn if any of them are likely to be affected by optical loading, stray light or are likely aliases of a bright source.

In 2SXPS, this marked the end of the individual dataset processing. For LSXPS, the dataset is then subjected to the transient search process detailed in Section 4, and then the results are stored in the LSXPS cache.

APPENDIX B: CATALOGUE TABLES

There are seven tables available for download, the contents of which are described below. These tables are:

- Sources
- Datasets
- Detections
- ObsSources
- External catalogue matches
- Old Stacks
- Transients

³¹ Stray light is only freely fitted to the total-band image of single observations. For the sub-bands the position of the stray-light source is fixed, but the normalisation can vary. For stacked images the stray light definitions are taken from the individual observations' results, and only the normalisation is free to vary, even in the total band

³² https://heasarc.gsfc.nasa.gov/docs/heasarc/caldb/swift/docs/xrt/SWIFT-XRT-CALDB-10_v01.pdf

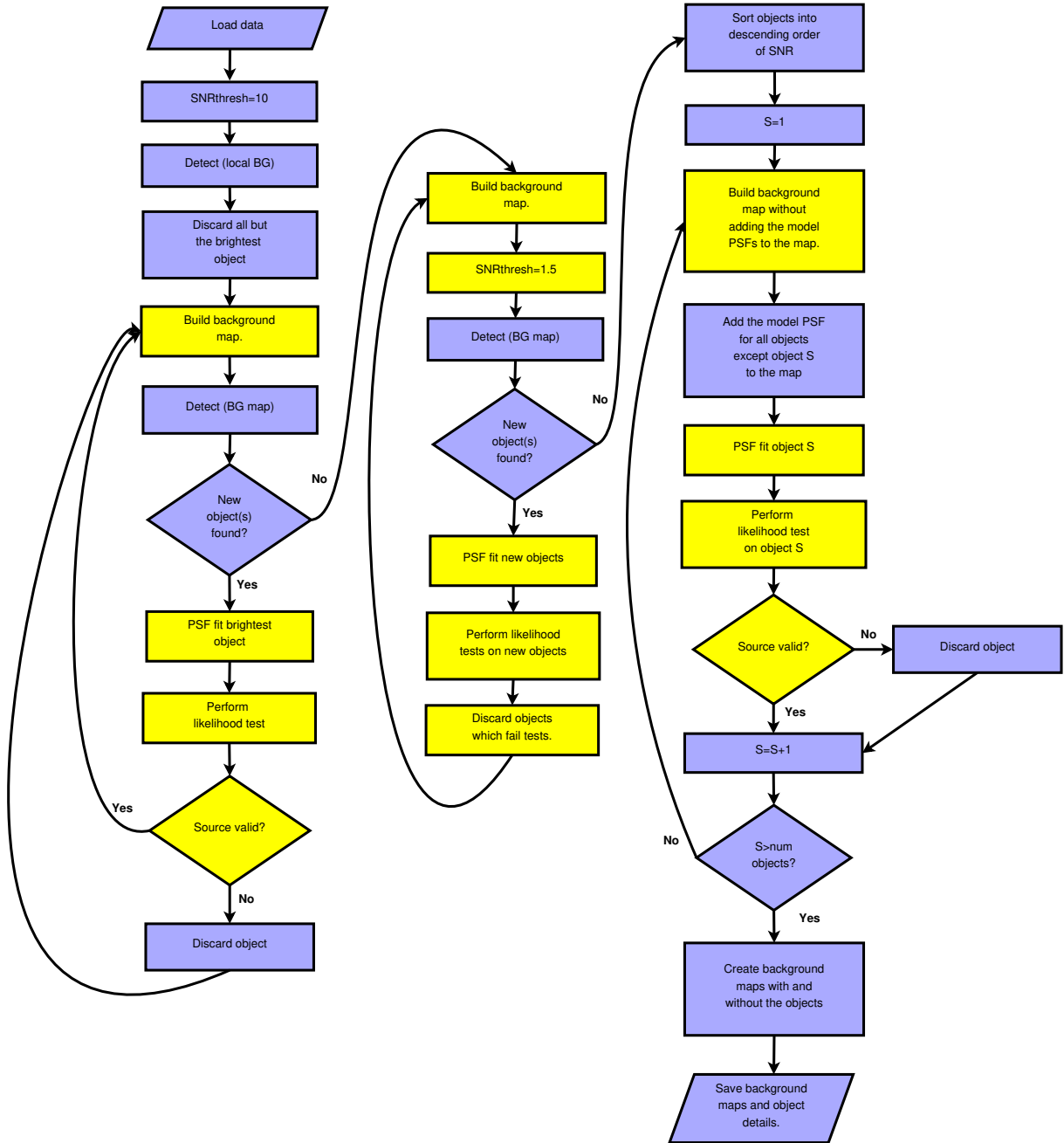


Figure A1. Diagrammatic outline of the source detection mechanism, reproduced from fig 2 of Evans et al. (2020)

In the following sections we give for each a short description and then a list of all of the table columns.

Many of the properties in the tables have errors associated with them; these are given in two extra columns with ‘_pos’ and ‘_neg’ added to the column names, e.g. the column ‘Rate’ is followed by ‘Rate_pos’ and ‘Rate_neg’. Rather than list all of these columns (the tables are long enough. . .), the tables below include the field ‘Has Errors?’ If this is ‘Yes’ it indicates that these extra columns exist as well. These errors are all $1-\sigma$ errors and assume a Gaussian distribution. A value of ‘[bool]’ in the units column indicates that the field is boolean.

B1 Sources

The ‘Sources’ table is the main LSXPS table, containing details of all of the unique sources in LSXPS. Note that sources can be removed from this table as the catalogue evolves, as well as being added to it (see Section 3.2).

Table B1: Contents of the ‘Sources’ database table.

Field	Units	Description	Has Errors?
LSXPS_ID		Numerical unique source identifier within LSXPS.	
IAUName		IAU-format name, LSXPS JHHMMSS+-ddmmsss. <i>Name and position</i>	
RA	Deg	Right Ascension (J2000) in decimal degrees.	
Decl	Deg	Declination (J2000) in decimal degrees.	
Err90	arcsec	Position uncertainty, 90% confidence, radial, assumed to be Rayleigh-distributed.	
AstromType		Provenance of source astrometry. 0=Swift star tracker, 1=XRT/2MASS astrometry.	
l	Deg	Galactic longitude.	
b	Deg	Galactic latitude.	
MeanOffAxisAngle	arcmin	The mean angular distance of the source from the XRT boresight in all observations within which the source was detected (arcmin).	
NearestNeighbour	arcsec	The distance to the closest LSXPS source to this one.	
NearestOKNeighbour	arcsec	The distance to the closest LSXPS source to this one which is ranked Good or Reasonable and has no other DetFlag bits set.	
NearestNeighbour_ID		The LSXPS_ID of the closest LSXPS source to this one.	
NearestOKNeighbour_ID		The LSXPS_ID of the closest LSXPS source to this one which is ranked Good or Reasonable and has no other DetFlag bits set.	
HPPIX		The Healpix pixel containing the source (NSIDE=128, ordering=RING). <i>Exposure details</i>	
Exposure	s	The total exposure at the source location in the catalogue.	
FirstObsDate		The UTC date & time of the start of the first observation in LSXPS which covered the source location.	
LastObsDate		The UTC date & time of the end of the last observation in LSXPS which covered the source location.	
FirstObsMET	MET	The time of the start of the first observation in LSXPS which covered the source location, in Swift Mission Elapsed Time.	
LastObsMET	MET	The time of the end of the last observation in LSXPS which covered the source location in, Swift Mission Elapsed Time.	
FirstDetDate		The UTC date & time of the start of the first observation in LSXPS in which the source count rate is inconsistent with 0 at the 3- σ level.	
LastDetDate		The UTC date & time of the end of the last observation in LSXPS in which the source count rate is inconsistent with 0 at the 3- σ level.	
FirstDetMET	MET	The time of the start of the first observation in LSXPS in which the source count rate is inconsistent with 0 at the 3- σ level, in Swift Mission Elapsed Time.	
LastDetMET	MET	The time of the end of the last observation in LSXPS in which the source count rate is inconsistent with 0 at the 3- σ level, in Swift Mission Elapsed Time.	
FirstBlindDetDate		The UTC date & time of the start of the first	

Continued. . .

Table B1 – continued from previous page

Field	Units	Description	Has Errors?
LastBlindDetDate		observation in LSXPS in which the source is detected in the blind search.	
FirstBlindDetMET	MET	The UTC date & time of the end of the last observation in LSXPS in which the source is detected in the blind search.	
LastBlindDetMET	MET	The time of the start of the first observation in LSXPS in which the source is detected in the blind search, in Swift Mission Elapsed Time.	
NumObs		The time of the end of the last observation in LSXPS in which the source is detected in the blind search, in Swift Mission Elapsed Time.	
NumBlindDetObs		The number of observations covering the position of this source.	
NumDetObs		The number of observations in which this source was found in a blind search.	
BestDetectionID		The number of observations in which this source is detected.	
NonBlindDet_band0		The ID of the 'best' detection, (cf the detections table).	
NonBlindDet_band1		Whether the count-rate in the 0.3–10 keV band is inconsistent with 0 at the 3- σ level.	
NonBlindDet_band2		Whether the count-rate in the 0.3–1 keV band is inconsistent with 0 at the 3- σ level.	
NonBlindDet_band3		Whether the count-rate in the 1–2 keV band is inconsistent with 0 at the 3- σ level.	
		Whether the count-rate in the 2–10 keV band is inconsistent with 0 at the 3- σ level.	
		<i>Quality flag parameters</i>	
DetFlag		The final source detection flag.	
FieldFlag		The final fieldFlag for this source.	
DetFlag_band0		The final detection flag the 0.3–10 keV band.	
DetFlag_band1		The final detection flag the 0.3–1 keV band.	
DetFlag_band2		The final detection flag in the 1–2 keV band.	
DetFlag_band3		The final detection flag in the 2–10 keV band.	
OpticalLoadingWarning		The worst optical loading warning from all detections of this source. If this is 0 there is no warning, otherwise there is a nearby optical source brighter than the level at which optical loading becomes a concern; the value indicates how many magnitudes brighter than that level the source is.	
StrayLightWarning		Whether any detection of this source occurred within fitted stray light rings.	
NearBrightSourceWarning		Whether any detection of this source occurred within the PSF wings of a bright object.	
IsPotentialAlias		Whether this source is potentially an alias (i.e. duplicate) of another source.	
		<i>Processing details</i>	
WhenAdded		The date at which this source was added to LSXPS.	
StillDetected		Whether the source was detected in the most recent observation of its location (1=yes; 0=no, but last upper limit unconstraining; -1 = no, and upper limit below last detection).	
ProcessedStatus		A bit-wise flag describing the processing status of the source data.	
WhenModified		The date at which this source was last analysed.	
		<i>Count rate and variability measurements</i>	

Continued. . .

Table B1 – continued from previous page

Field	Units	Description	Has Errors?
Rate_band0	s ⁻¹	The mean count-rate in the 0.3–10 keV band.	Yes
HR1		The aggregate HR1 hardness ratio of the source.	Yes
HR2		The aggregate HR2 hardness ratio of the source.	Yes
Rate_band1	s ⁻¹	The mean count-rate in the 0.3–1 keV band.	Yes
Rate_band2	s ⁻¹	The mean count-rate in the 1-2 keV band.	Yes
Rate_band3	s ⁻¹	The mean count-rate in the 2–10 keV band.	Yes
Counts_band0		The total number of counts in the source region in the 0.3–10 keV band.	
Counts_band1		The total number of counts in the source region in the 0.3–1 keV band.	
Counts_band2		The total number of counts in the source region in the 1-2 keV band.	
Counts_band3		The total number of counts in the source region in the 2–10 keV band.	
BgCounts_band0		The total number of background counts expected in the source region in the 0.3–10 keV band.	
BgCounts_band1		The total number of background counts expected in the source region in the 0.3–1 keV band.	
BgCounts_band2		The total number of background counts expected in the source region in the 1-2 keV band.	
BgCounts_band3		The total number of background counts expected in the source region in the 2–10 keV band.	
RateCF_band0	s ⁻¹	The PSF correction factor in the 0.3–10 keV band.	
RateCF_band1	s ⁻¹	The PSF correction factor in the 0.3–1 keV band.	
RateCF_band2	s ⁻¹	The PSF correction factor in the 1-2 keV band.	
RateCF_band3	s ⁻¹	The PSF correction factor in the 2–10 keV band.	
UL_band0	s ⁻¹	The 3- σ upper confidence limit on the count-rate in the 0.3–10 keV band.	
UL_band1	s ⁻¹	The 3- σ upper confidence limit on the count-rate in the 0.3–1 keV band.	
UL_band2	s ⁻¹	The 3- σ upper confidence limit on the count-rate in the 1-2 keV band.	
UL_band3	s ⁻¹	The 3- σ upper confidence limit on the count-rate in the 2–10 keV band.	
PeakRate_band0	s ⁻¹	The peak count-rate in the 0.3–10 keV band.	Yes
PeakRate_band1	s ⁻¹	The peak count-rate in the 0.3–1 keV band.	Yes
PeakRate_band2	s ⁻¹	The peak count-rate in the 1-2 keV band.	Yes
PeakRate_band3	s ⁻¹	The peak count-rate in the 2–10 keV band.	Yes
<i>Flux measurements and spectral parameters</i>			
GalacticNH	cm ⁻²	The Galactic absorption column in the direction of the source, from Willingale et al (2013), in cm ⁻² .	
PvarPchiSnapshot_band0		The probability that the source count-rate in the 0.3–10 keV band does not vary between snapshots.	
PvarPchiSnapshot_band1		The probability that the source count-rate in the 0.3–1 keV band does not vary between snapshots.	
PvarPchiSnapshot_band2		The probability that the source count-rate in the 1-2 keV band does not vary between snapshots.	
PvarPchiSnapshot_band3		The probability that the source count-rate in the 2–10 keV band does not vary between snapshots.	
PvarPchiSnapshot_HR1		The probability that the source HR1 hardness ratio does not vary between snapshots.	
PvarPchiSnapshot_HR2		The probability that the source HR2 hardness ratio does not vary between snapshots.	
PvarPchiObsID_band0		The probability that the source count-rate in the 0.3–10 keV band does not vary between	

Continued. . .

Table B1 – continued from previous page

Field	Units	Description	Has Errors?
PvarPchiObsID_band1		observations. The probability that the source count-rate in the 0.3–1 keV band does not vary between observations.	
PvarPchiObsID_band2		The probability that the source count-rate in the 1–2 keV band does not vary between observations.	
PvarPchiObsID_band3		The probability that the source count-rate in the 2–10 keV band does not vary between observations.	
PvarPchiObsID_HR1		The probability that the source HR1 hardness ratio does not vary between observations.	
PvarPchiObsID_HR2		The probability that the source HR2 hardness ratio does not vary between observations.	
<i>Flux measurements and spectral parameters</i>			
WhichPow		Which method of determining the spectral properties assuming a power-law was used: 0=Canned spectrum, 1=Interpolated from the HR, 2=Spectrum constructed and fitted.	
WhichAPEC		Which method of determining the spectral properties assuming an APEC was used: 0=Canned spectrum, 1=Interpolated from the HR, 2=Spectrum constructed and fitted.	
PowECFO	erg cm ⁻² ct ⁻¹	The Energy Conversion Factor from 0.3–10 keV count-rate to 0.3–10 keV observed flux, assuming a power-law spectrum.	
PowECFU	erg cm ⁻² ct ⁻¹	The Energy Conversion Factor from 0.3–10 keV count-rate to 0.3–10 keV unabsorbed flux, assuming a power-law spectrum.	
PowFlux	erg cm ⁻² s ⁻¹	The mean 0.3–10 keV observed flux assuming a power-law spectrum.	Yes
PowUnabsFlux	erg cm ⁻² s ⁻¹	The mean 0.3–10 keV unabsorbed flux assuming a power-law spectrum.	Yes
APECECFO	erg cm ⁻² ct ⁻¹	The Energy Conversion Factor from 0.3–10 keV count-rate to 0.3–10 keV observed flux, assuming an APEC spectrum.	Yes
APECECFU	erg cm ⁻² ct ⁻¹	The Energy Conversion Factor from 0.3–10 keV count-rate to 0.3–10 keV unabsorbed flux, assuming an APEC spectrum.	Yes
APECFlux	erg cm ⁻² s ⁻¹	The mean 0.3–10 keV observed flux assuming an APEC spectrum.	Yes
APECUnabsFlux	erg cm ⁻² s ⁻¹	The mean 0.3–10 keV unabsorbed flux assuming an APEC spectrum.	Yes
PowPeakFlux	erg cm ⁻² s ⁻¹	The peak 0.3–10 keV observed flux assuming a power-law spectrum.	Yes
PowPeakUnabsFlux	erg cm ⁻² s ⁻¹	The peak 0.3–10 keV unabsorbed flux assuming a power-law spectrum.	Yes
APECPeakFlux	erg cm ⁻² s ⁻¹	The peak 0.3–10 keV observed flux assuming an APEC spectrum.	Yes
APECPeakUnabsFlux	erg cm ⁻² s ⁻¹	The peak 0.3–10 keV unabsorbed flux assuming an APEC spectrum.	Yes
FixedPowECFO	erg cm ⁻² ct ⁻¹	The Energy Conversion Factor from 0.3–10 keV count-rate to 0.3–10 keV observed flux, assuming the canned power-law spectrum.	Yes
FixedPowECFU	erg cm ⁻² ct ⁻¹	The Energy Conversion Factor from 0.3–10 keV count-rate to 0.3–10 keV unabsorbed flux, assuming the canned power-law spectrum.	Yes
FixedPowFlux	erg cm ⁻² s ⁻¹	The mean 0.3–10 keV observed flux assuming the	Yes

Continued...

Table B1 – continued from previous page

Field	Units	Description	Has Errors?
FixedPowUnabsFlux	$\text{erg cm}^{-2} \text{s}^{-1}$	canned power-law spectrum. The mean 0.3–10 keV unabsorbed flux assuming the canned power-law spectrum.	Yes Yes Yes
FixedAPECECFO	$\text{erg cm}^{-2} \text{ct}^{-1}$	The Energy Conversion Factor from 0.3–10 keV count-rate to 0.3–10 keV observed flux, assuming the canned APEC spectrum.	
FixedAPECECFU	$\text{erg cm}^{-2} \text{ct}^{-1}$	The Energy Conversion Factor from 0.3–10 keV count-rate to 0.3–10 keV unabsorbed flux, assuming the canned APEC spectrum.	
FixedAPECFlux	$\text{erg cm}^{-2} \text{s}^{-1}$	The mean 0.3–10 keV observed flux assuming the canned APEC spectrum.	Yes Yes
FixedAPECUnabsFlux	$\text{erg cm}^{-2} \text{s}^{-1}$	The mean 0.3–10 keV unabsorbed flux assuming the canned APEC spectrum.	Yes Yes
InterpPowECFO	$\text{erg cm}^{-2} \text{ct}^{-1}$	The Energy Conversion Factor from 0.3–10 keV count-rate to 0.3–10 keV observed flux, assuming the power-law spectrum interpolated from the HRs.	
InterpPowECFU	$\text{erg cm}^{-2} \text{ct}^{-1}$	The Energy Conversion Factor from 0.3–10 keV count-rate to 0.3–10 keV unabsorbed flux, assuming the power-law spectrum interpolated from the HRs.	
InterpPowNH	cm^{-2}	The hydrogen column density inferred assuming the power-law spectrum interpolated from the HRs.	Yes Yes
InterpPowGamma		The spectral photon index inferred assuming the power-law spectrum interpolated from the HRs.	Yes
InterpPowFlux	$\text{erg cm}^{-2} \text{s}^{-1}$	The mean 0.3–10 keV observed flux assuming the power-law spectrum interpolated from the HRs.	Yes Yes
InterpPowUnabsFlux	$\text{erg cm}^{-2} \text{s}^{-1}$	The mean 0.3–10 keV unabsorbed flux assuming the power-law spectrum interpolated from the HRs.	Yes Yes
InterpAPECECFO	$\text{erg cm}^{-2} \text{ct}^{-1}$	The Energy Conversion Factor from 0.3–10 keV count-rate to 0.3–10 keV observed flux, assuming the APEC spectrum interpolated from the HRs.	
InterpAPECECFU	$\text{erg cm}^{-2} \text{ct}^{-1}$	The Energy Conversion Factor from 0.3–10 keV count-rate to 0.3–10 keV unabsorbed flux, assuming the APEC spectrum interpolated from the HRs.	
InterpAPECNH	cm^{-2}	The hydrogen column density inferred assuming the APEC spectrum interpolated from the HRs.	Yes Yes
InterpAPECkT	keV	The temperature inferred assuming the APEC spectrum interpolated from the HRs.	Yes Yes
InterpAPECFlux	$\text{erg cm}^{-2} \text{s}^{-1}$	The mean 0.3–10 keV observed flux assuming the APEC spectrum interpolated from the HRs.	Yes Yes
InterpAPECUnabsFlux	$\text{erg cm}^{-2} \text{s}^{-1}$	The mean 0.3–10 keV unabsorbed flux assuming the APEC spectrum interpolated from the HRs.	Yes Yes
P_pow		The probability that the HR values of this source could be obtained if the true spectrum is an absorbed power-law.	
P_APEC		The probability that the HR values of this source could be obtained if the true spectrum is an APEC.	
FittedPowECFO	$\text{erg cm}^{-2} \text{ct}^{-1}$	The Energy Conversion Factor from 0.3–10 keV count-rate to 0.3–10 keV observed flux, assuming the power-law spectral model fitted to a custom-built spectrum.	
FittedPowECFU	$\text{erg cm}^{-2} \text{ct}^{-1}$	The Energy Conversion Factor from 0.3–10 keV count-rate to 0.3–10 keV unabsorbed flux, assuming the power-law spectral model fitted to a custom-built spectrum.	

Continued. . .

Table B1 – continued from previous page

Field	Units	Description	Has Errors?
FittedPowNH	cm^{-2}	The hydrogen column density inferred assuming the power-law spectral model fitted to a custom-built spectrum.	Yes
FittedPowGamma		The spectral photon index inferred assuming the power-law spectral model fitted to a custom-built spectrum.	Yes
FittedPowFlux	$\text{erg cm}^{-2} \text{s}^{-1}$	The mean 0.3–10 keV observed flux assuming the power-law spectral model fitted to a custom-built spectrum.	Yes
FittedPowUnabsFlux	$\text{erg cm}^{-2} \text{s}^{-1}$	The mean 0.3–10 keV unabsorbed flux assuming the power-law spectral model fitted to a custom-built spectrum.	Yes
FittedPowCstat		The C-statistic from the power-law spectral fit to the custom-built spectrum.	Yes
FittedPowDOF		The number of degrees of freedom in the power-law spectral fit to the custom-built spectrum.	Yes
FittedPowReducedChi2		The Churazov-weighted reduced χ^2 from the power-law spectral fit to the custom-built spectrum.	Yes
FittedAPECECFO	$\text{erg cm}^{-2} \text{ct}^{-1}$	The Energy Conversion Factor from 0.3–10 keV count-rate to 0.3–10 keV observed flux, assuming the APEC spectral model fitted to a custom-built spectrum.	Yes
FittedAPECECFU	$\text{erg cm}^{-2} \text{ct}^{-1}$	The Energy Conversion Factor from 0.3–10 keV count-rate to 0.3–10 keV unabsorbed flux, assuming the APEC spectral model fitted to a custom-built spectrum.	Yes
FittedAPECNH	cm^{-2}	The hydrogen column density inferred assuming the APEC spectral model fitted to a custom-built spectrum.	Yes
FittedAPECKT	keV	The temperature inferred assuming the APEC spectral model fitted to a custom-built spectrum.	Yes
FittedAPECFflux	$\text{erg cm}^{-2} \text{s}^{-1}$	The mean 0.3–10 keV observed flux assuming the APEC spectral model fitted to a custom-built spectrum.	Yes
FittedAPECUabsFlux	$\text{erg cm}^{-2} \text{s}^{-1}$	The mean 0.3–10 keV unabsorbed flux assuming the APEC spectral model fitted to a custom-built spectrum.	Yes
FittedAPECCstat		The C-statistic from the APEC spectral fit to the custom-built spectrum.	Yes
FittedAPECDOF		The number of degrees of freedom in the APEC spectral fit to the custom-built spectrum.	Yes
FittedAPECRducedChi2		The Churazov-weighted reduced χ^2 from the APEC spectral fit to the custom-built spectrum.	Yes
HasSpec	[bool]	Whether a custom-built spectrum was created for this source.	
<i>External catalogue cross-correlation results</i>			
NumExternalMatches	[bool]	The number of external sources found to agree spatially with this one at the 3- σ level.	
NumExternalMatches_slim	[bool]	The number of external sources found to agree spatially with this one at the 3- σ level, excluding 2MASS, USNO-B1 and ALLWISE matches.	
MatchInROSHRI	[bool]	Whether the source is spatially within 3 σ of a source in the Rosat HRI catalogue.	
MatchIn2RXS	[bool]	Whether the source is spatially within 3 σ of a source in the 2RXS catalogue.	
MatchIn4XMM_DR10	[bool]	Whether the source is spatially within 3 σ of a	

Continued. . .

Table B1 – continued from previous page

Field	Units	Description	Has Errors?
MatchIn4XMM_DR10s	[bool]	source in the 3XMM-DR8 catalogue. Whether the source is spatially within 3σ of a source in the 3XMM-DR7s (stacked) catalogue.	
MatchInXMMSL2	[bool]	Whether the source is spatially within 3σ of a source in the XMMSL2 catalogue.	
MatchInSwiftFT	[bool]	Whether the source is spatially within 3σ of a source in the SwiftFT catalogue.	
MatchIn1SWXRT	[bool]	Whether the source is spatially within 3σ of a source in the 1SWXRT catalogue.	
MatchInXRTGRB	[bool]	Whether the source is spatially within 3σ of an XRT GRB afterglow.	
MatchInSDSS_QSO_DR14	[bool]	Whether the source is spatially within 3σ of a source in the SDSS QSO DR14 catalogue.	
MatchIn2MASS	[bool]	Whether the source is spatially within 3σ of a source in the 2MASS catalogue.	
MatchInUSNOB1	[bool]	Whether the source is spatially within 3σ of a source in the USNO-B1 catalogue.	
MatchIn2CSC	[bool]	Whether the source is spatially within 3σ of a source in the 2CSC catalogue.	
MatchIn2SXPS	[bool]	Whether the source is spatially within 3σ of a source in the 2SXPS catalogue.	

B2 Datasets

The ‘Datasets’ table contains information about every dataset (observations and stacked image) in LSXPS. Observations, once in this table, will not be removed. Stacked images may be removed as a newer version of a stack is added. If a stack is superseded, the final version of it will remain in this table (see Section 3.3).

Table B2: Contents of the ‘Datasets’ database table.

Field	Units	Description	Has Errors?
DatasetID		The unique identifier for this dataset.	
ObsID		The identifier of the observation or stacked image in which this detection occurred.	
DataVersion		The version of this dataset; for stacked images it is the number of times the image has been analysed with extra data; for single observations it is the number of times the original data were processed after data downlink.	
IsStackedImage	[bool]	Whether or not this is a stacked image.	
FieldFlag		The warning flag associated with this field.	
RA	Deg	The Right Ascension (J2000) of the field centre in decimal degrees.	
Decl	Deg	The declination (J2000) of the field centre in decimal degrees.	
l	Deg	Galactic longitude of the field centre.	
b	Deg	Galactic latitude of the field centre.	
ImageSize		The side length of the field image in XRT pixels (2.357 arcsec per pixel).	
ExposureUsed	s	The nominal exposure in the dataset, after all screening has been carried out.	
StartTime_UTC	UTC	The UTC start time of the dataset.	
StopTime_UTC	UTC	The UTC end time of the dataset.	
OriginalExposure	s	The original nominal exposure in the dataset before screening.	
StartTime_MET	MET	The start time of the dataset, in Swift Mission Elapsed Time.	
StopTime_MET	MET	The end time of the dataset, in Swift Mission Elapsed Time.	
MidTime_MET	MET	The mid-time of the dataset, in Swift Mission Elapsed Time.	
MidTime_TDB		The mid-time of the dataset, in Barycentric Dynamical Time.	
MidTime_MJD		The mid-time of the dataset, as a Modified Julian Date.	
LiveDate	UTC	The UTC date at which this dataset became live.	
FieldBG_band0	ct s ⁻¹ pixel ⁻¹	The mean background level in the 0.3–10 keV band.	
FieldBG_band1	ct s ⁻¹ pixel ⁻¹	The mean background level in the 0.3–1 keV band.	
FieldBG_band2	ct s ⁻¹ pixel ⁻¹	The mean background level in the 1–2 keV band.	
FieldBG_band3	ct s ⁻¹ pixel ⁻¹	The mean background level in the 2–10 keV band.	
NumSrc_band0		The number of sources detected in this dataset in the 0.3–10 keV band.	
NumOK_band0		The number of good or reasonable sources detected in this dataset in the 0.3–10 keV band.	
MedianDist_band0		The median distance between sources detected in this dataset in the 0.3–10 keV band.	
NumSrc_band1		The number of sources detected in this dataset in the 0.3–1 keV band.	
NumOK_band1		The number of good or reasonable sources detected in this dataset in the 0.3–1 keV band.	
MedianDist_band1		The median distance between sources detected in	

Continued. . .

Table B2 – continued from previous page

Field	Units	Description	Has Errors?
NumSrc_band2		this dataset in the 0.3–1 keV band. The number of sources detected in this dataset in the 1-2 keV band.	
NumOK_band2		The number of good or reasonable sources detected in this dataset in the 1-2 keV band.	
MedianDist_band2		The median distance between sources detected in this dataset in the 1-2 keV band.	
NumSrc_band3		The number of sources detected in this dataset in the 2–10 keV band.	
NumOK_band3		The number of good or reasonable sources detected in this dataset in the 2–10 keV band.	
MedianDist_band3		The median distance between sources detected in this dataset in the 2–10 keV band.	
NumberOfSnapshots		The number of snapshots contributing to this dataset.	
AstromError		The 90% confidence radial uncertainty on the XRT-2MASS astrometric correction.	
CRVAL1_corr		The CRVAL1 WCS reference value for the dataset derived from the XRT-2MASS astrometric correction.	
CRVAL2_corr		The CRVAL2 WCS reference value for the dataset derived from the XRT-2MASS astrometric correction.	
CROTA2_corr		The CROTA1 WCS reference value for the dataset derived from the XRT-2MASS astrometric correction.	
IsObsoleteStack	[bool]	Whether this corresponds to a stacked image which has been superseded by a newer version, but which contains a unique detection of a source.	

B3 Detections

The ‘Detections’ table contains the information about every individual detection in every band, before these are combined to create sources.

Table B3: Contents of the ‘Detections’ database table.

Field	Units	Description	Has Errors?
DetectionID		A unique identifier for this detection.	
DatasetID		The unique identifier for the dataset in which the detection occurred.	
ObsID		The obsID of the observation in which the detection occurred.	
ObsSourceID		The ID of the obsSource this detection is part of.	
SourceNo		The identifier of this source within this obsid and band.	
Band		The energy band (0-3) in which this detection occurred.	
CorrectedExposure	s	The exposure time at the position of the source in this obsID.	
ExposureFraction	s	The fractional exposure at the position of this source, i.e. the exposure divided by the nominal exposure for the field.	
OffaxisAngle	arcmin	The angular distance of the source from the XRT boresight in all observations within which the source was detected .	
RA	Deg	Right Ascension (J2000) in decimal degrees.	Yes
Decl	Deg	Declination (J2000) in decimal degrees.	Yes
Err90	arcsec	Position uncertainty, 90% confidence, radial, assumed to be Rayleigh-distributed.	
RA_corrected	Deg	Right Ascension (J2000) in decimal degrees corrected using XRT-2MASS astrometry.	
Decl_corrected	Deg	Declination (J2000) in decimal degrees corrected using XRT-2MASS astrometry.	
Err90_corrected	arcsec	Uncertainty on the corrected position, 90% confidence, radial, assumed to be Rayleigh-distributed.	
l	Deg	Galactic longitude.	
b	Deg	Galactic latitude.	
l_corrected	Deg	Galactic longitude corrected using XRT-2MASS astrometry.	
b_corrected	Deg	Galactic latitude corrected using XRT-2MASS astrometry.	
IMG_X		The x position of the object in the SKY image plane.	
IMG_Y		The y position of the object in the SKY image plane.	
NearestNeighbour	arcsec	The distance to the closest detection to this one, in this image.	
NearestOKNeighbour	arcsec	The distance to the closest Good or Reasonable detection to this one, in this image.	
DetFlag		The detection flag for this detection.	
OpticalLoadingWarning		Whether this detection is potentially affected by optical loading. If this is 0 there is no catalogue bright optical source nearby, otherwise there is a nearby optical source brighter than the level at which optical loading becomes a concern; the value indicates how many magnitudes brighter than that level the source is.	
StrayLightWarning		Whether this detection occurred within fitted	

Continued. . .

Table B3 – continued from previous page

Field	Units	Description	Has Errors?
NearBrightSourceWarning		stray light rings. Whether this detection occurred within the PSF wings of a fitted bright source.	
MatchesKnownExtended	[bool]	Whether the position of this source matches a known extended X-ray source.	
PileupFitted		Whether the accepted fit included pile up.	
SNR		The signal to noise ratio of the detection.	
CtsInPSFFit		Number of counts in the image region over which the final PSF fit was performed.	
BGRateInPSFFit	s ⁻¹	Mean count-rate in the background map in the region over which the final PSF fit was performed.	
Cstat		The C-statistic value from the PSF fit.	
Cstat_nosrc		The C-statistic value derived over the PSF fit region if no source is fitted.	
L_src		The log-likelihood value that this detection is not just a background fluctuation.	
Cstat_flat		The Cstat value found from a fit assuming a constant increase above the background (i.e. the count excess is flat, not PSF-like).	
Lflat		The log-likelihood value that this detection is PSF like, not a flat count increase.	
FracPix		The fraction of pixels within the PSF fit region which are exposed.	
Pileup_S		The best-fitting S parameter of the pile-up model, if fitted.	
Pileup_l		The best-fitting l parameter of the pile-up model, if fitted.	
Pileup_c		The best-fitting c parameter of the pile-up model, if fitted.	
Pileup_tau		The best-fittingtau parameter of the pile-up model, if fitted.	
Cstat_altPileup		The Cstat value found from the unusued fit. i.e. if the piled up model was used, this gives the Cstat from the non-piled-up fit, and vice-versa.	
PSF_Fit_Radius		The radius of the circular region over which PSF fitting was carried out (in image pixels, 2.357'' to a side).	
CellDetect_BoxWidth		The full width of the cell-detect box in which this source was detected (in image pixels, 2.357'' to a side).	
Rate	s ⁻¹	The corrected count-rate of this detection (i.e. in the band of this image).	Yes
CtsInRate	s ⁻¹	The total number of counts in the region used to extract the count rate.	Yes
BGCtsInRate	s ⁻¹	The total number of counts in the region used to extract the count rate.	
Rate_CF	s ⁻¹	The PSF correction factor for the count rate.	
BGRateInRate	s ⁻¹	The background rate in the region used for count-rate calculation.	

B4 ObsSources

As described in Appendix A, the process of identifying unique sources has two steps. In the first, individual detections from different bands within a dataset are merged to identify the objects uniquely detected in that dataset. These are referred to as *ObsSources* and are available in this catalogue table.

Table B4: Contents of the ‘ObsSource’ database table.

Field	Units	Description	Has Errors?
ObsSourceID		The unique identifier of this ObsSource.	
DatasetID		The dataset identifier in which this obsSource was found.	
LSXPS_ID		Numerical unique source identifier within LSXPS.	
OSNum		The identifier of this obsSource within this dataset.	
UsedCorrectedPosition	[bool]	Whether or not the astrometrically-corrected position of this obsSource should be used.	
NearestNeighbour	arcsec	The distance to the closest LSXPS obsSource within this dataset.	
NearestOKNeighbour	arcsec	The distance to the closest good or reasonable LSXPS obsSource within this dataset.	
Exposure	s	The exposure time at the position of the obsSource, corrected for vignetting.	
HR1		The aggregate HR1 hardness ratio of the obsSource.	Yes
HR2		The aggregate HR2 hardness ratio of the obsSource.	Yes
BestBand		The energy band corresponding to the best detection of this obsSource in this dataset.	Yes
PileupWarning	[bool]	Whether a pile up warning exists, indicating that the object is very piled up and in some bands there is evidence of pile up not being fitted.	
BestDetectionID		The DetectionID of the best detection of this obsSource in this dataset.	
IsOrphanSource	[bool]	Whether this source is one which is only detected in this dataset, and this dataset is deprecated.	

B5 External catalogue matches

As with previous SXPS catalogues, we check each source for possible counterparts in other catalogues. Details of those matches are given in this table, which is entitled ‘xCorr’ in the file names, for brevity.

Table B5: Contents of the ‘xCorr’ database table.

Field	Units	Description	Has Errors?
LSXPS_ID		The numerical identifier of the LSXPS source.	
ExtCat_ID		The catalogued name of the external source.	
Catalogue		The catalogue in which the external source was found.	
Distance	arcsec	The distance in arcseconds between the 2SXPS and external source positions.	
Ext_RA	Deg	The Right Ascension (J2000) in decimal degrees of the external source.	
Ext_Decl	Deg	The declination (J2000) in decimal degrees of the external source.	
Ext_Err90	arcsec	The 90% confidence radial position error of the external source used for cross correlation. This may have been converted to 90% (assuming Rayleigh statistics) and had a systematic error added if necessary, therefore may differ from the catalogued value.	

B6 OldStacks

When a new version of a stacked image is processed, or the stack superseded (see Section 3.3), some brief information about the old version is stored in this table.

Table B6: Contents of the ‘oldStacks’ database table.

Field	Units	Description	Has Errors?
DatasetID		The unique identifier for this dataset.	
DataVersion		The version of this dataset; for stacked images it is the number of times the image has been analysed with extra data; for single observations it is the number of times the original data were processed after data downlink.	
LiveDate	UTC	The UTC date at which this dataset became live.	
ObsID		The identifier of the observation or stacked image in which this detection occurred.	
IsObsoleteStack	[bool]	Whether this corresponds to a stacked image which has been superseded by a newer version, but which contains a unique detection of a source.	

B7 Transients

The ‘Transients’ table contains the information about every transient counterpart that has been checked by a member of the XRT team and classed into one of the ‘possible transient’ categories (Section 4).

Table B7: Contents of the ‘Transients’ database table.

Field	Units	Description	Has Errors?
TransientID		A unique numerical identifier for this transient within this catalogue.	
IAUName		The IAU-format name of the transient: SwiftJ HHMMSS.S+ddmmss.	
LSXPS_ID		The source identifier within the main LSXPS catalogue.	
LSXPSName		The IAU name of this object in the main LSXPS catalogue.	
Classification		A numerical code describing how this transient has been classified.	
RA	Deg	Right Ascension (J2000) in decimal degrees.	
Decl	Deg	Declination (J2000) in decimal degrees.	
Err90	arcsec	Position uncertainty, 90% confidence, radial, assumed to be Rayleigh-distributed.	
l	Deg	Galactic longitude.	
b	Deg	Galactic latitude.	
DiscoveryDatasetID		The date of the observation in which the transient was first found.	
ObsSourceID		The numerical identifier of the first detection in the Public_ObsSources table.	
PeakRateAtDetection	s ⁻¹	The peak count-rate in the 0.3–10 keV band in the dataset in which the transient was first detected.	Yes
PeakSoftMedBandRateAtDetection	s ⁻¹	The peak count-rate in the 0.3–2 keV band in the dataset in which the transient was first detected.	Yes
UpperLimitSource_Canned		Where the ‘best’ upper limit at the source location was taken from, where the ‘canned’ spectrum is used to convert between observatories.	
UpperLimitSource_DiscoverySpectrum		Where the ‘best’ upper limit at the source location was taken from, where the discovery spectrum is used to convert between observatories.	
UpperLimitSource_FullSpectrum		Where the ‘best’ upper limit at the source location was taken from, where the full spectrum is used to convert between observatories.	
Significance		How far above the best upper limit the peak count rate is, in Gaussian β .	
InitSpecNH	cm ⁻²	The hydrogen column density found in an automated power-law fit to a spectrum built from the discovery dataset.	
InitSpecGamma		The photon index found in an automated power-law fit to a spectrum built from the discovery dataset.	
InitSpecCstat		The C-statistic from an automated power-law fit to a spectrum built from the discovery dataset.	
InitSpecTestStat		The Churazov-weighted reduced χ^2 from an automated power-law fit to a spectrum built from the discovery dataset.	
InitSpecDof		The number of degrees of freedom in the automated power-law fit to a spectrum built from the	

Continued...

Table B7 – continued from previous page

Field	Units	Description	Has Errors?
FullSpecNH	cm^{-2}	discovery dataset. The hydrogen column density found in an automated power-law fit to a spectrum built from all observations of the transient after its discovery.	
FullSpecGamma		The photon index found in an automated power-law fit to a spectrum built from all observations of the transient after its discovery.	
FullSpecCstat		The C-statistic from an automated power-law fit to a spectrum built from all observations of the transient after its discovery.	
FullSpecTestStat		The Churazov-weighted reduced χ^2 from an automated power-law fit to a spectrum built from all observations of the transient after its discovery.	
FullSpecDof		The number of degrees of freedom in the automated power-law fit to a spectrum built from the all observations of the transient after its discovery.	
DiscoveryDate	UTC	The date of the analysis in which the transient was first found.	
DetectionDate	UTC	The MET of the observation in which the transient was first found.	
DetectionMET	MET	The date of the observation in which the transient was first found.	
LSXPS_UpperLimit	s^{-1}	An upper limit at the transient derived from the LSXPS catalogue.	
LSXPS_UpperLimit_ObsID		The observation in the LSXPS catalogue from which the upper limit was derived.	
XMM_UpperLimit_native	s^{-1}	An XMM-Newton upper limit at the transient location, obtained via the HILIGT server, in native XMM count-rate units.	
XMM_UpperLimit_ObsMode		The mode in which XMM was observing when the upper limit was obtained.	
XMM_UpperLimit_Instrument		The XMM-Newton instrument from which the upper limit was obtained.	
XMM_UpperLimit_asXRTTotal_DiscoverySpectrum	s^{-1}	The XMM-Newton upper limit converted to a 0.3–10 keV XRT count rate, using the automated power-law fit to a spectrum built from the discovery dataset.	
XMM_UpperLimit_asXRTTotal_FullSpectrum	s^{-1}	The XMM-Newton upper limit converted to a 0.3–10 keV XRT count rate, using the automated power-law fit to a spectrum built from the all observations of the transient after its discovery.	
XMM_UpperLimit_asXRTTotal_Canned	s^{-1}	The XMM-Newton upper limit converted to a 0.3–10 keV XRT count rate, using a standard AGN spectrum.	
RASS_UpperLimit_native	s^{-1}	An ROSAT All-Sky Survey upper limit at the transient location, obtained via the HILIGT server, in native ROSAT PSPC count-rate units.	
RASS_UpperLimit_asXRSoftMed_DiscoverySpectrum	s^{-1}	The RASS upper limit converted to a 0.3–2 keV XRT count rate, using the automated power-law fit to a spectrum built from the discovery dataset.	
RASS_UpperLimit_asXRSoftMed_FullSpectrum	s^{-1}	The RASS upper limit converted to a 0.3–2 keV XRT count rate, using the automated power-law fit to a spectrum built from the all observations of the transient after its discovery.	

Continued. . .

Table B7 – continued from previous page

Field	Units	Description	Has Errors?
RASS_UpperLimit_asXRTSoftMed_Canned	s ⁻¹	The RASS upper limit converted to a 0.3–2 keV XRT count rate, using a standard AGN spectrum.	
RASS_UpperLimit_asXRTTotal_DiscoverySpectrum	s ⁻¹	The RASS upper limit converted to a 0.3–10 keV XRT count rate, using the automated power-law fit to a spectrum built from the discovery dataset.	
RASS_UpperLimit_asXRTTotal_FullSpectrum	s ⁻¹	The RASS upper limit converted to a 0.3–10 keV XRT count rate, using the automated power-law fit to a spectrum built from the all observations of the transient after its discovery.	
RASS_UpperLimit_asXRTTotal_Canned	s ⁻¹	The RASS upper limit converted to a 0.3–10 keV XRT count rate, using a standard AGN spectrum.	
Notes		Any notes added by the XRT team.	